A Review of Gas Injection in Shale Reservoirs: Enhanced Oil/Gas Recovery Approaches and Greenhouse Gas Control

Fengshuang Du * and Bahareh Nojabaei

Mining and Minerals Engineering, Virginia Polytechnic Institute and State University, Blacksburg, VA 24060, USA; baharehn@vt.edu

* Correspondence: lindadu@vt.edu; Tel.: +1-540-449-8010

check for updates

Abstract: Shale oil and gas resources contribute significantly to the energy production in the U.S. Greenhouse gas emissions come from combustion of fossil fuels from potential sources of power plants, oil refineries, and flaring or venting of produced gas (primarily methane) in oilfields. Economic utilization of greenhouse gases in shale reservoirs not only increases oil or gas recovery, but also contributes to CO_2 sequestration. In this paper, the feasibility and efficiency of gas injection approaches, including huff-n-puff injection and gas flooding in shale oil/gas/condensate reservoirs are discussed based on the results of in-situ pilots, and experimental and simulation studies. In each section, one type of shale reservoir is discussed, with the following aspects covered: (1) Experimental and simulation results for different gas injection approaches; (2) mechanisms of different gas injection approaches; and (3) field pilots for gas injection enhanced oil recovery (EOR) and enhanced gas recovery (EGR). Based on the experimental and simulation studies, as well as some successful field trials, gas injection is deemed as a potential approach for EOR and EGR in shale reservoirs. The enhanced recovery factor varies for different experiments with different rock/fluid properties or models incorporating different effects and shale complexities. Based on the simulation studies and successful field pilots, CO_2 could be successfully captured in shale gas reservoirs through gas injection and huff-n-puff regimes. The status of flaring gas emissions in oilfields and the outlook of economic utilization of greenhouse gases for enhanced oil or gas recovery and CO_2 storage were given in the last section. The storage capacity varies in different simulation studies and is associated with well design, gas injection scheme and operation parameters, gas adsorption, molecular diffusion, and the modelling approaches.

Keywords: gas injection; shale oil reservoir; shale gas reservoir; shale condensate reservoir; enhanced oil/gas recovery; carbon dioxide sequestration

1. Introduction

Fossil fuels, including petroleum, natural gas, and coal, are the primary source of energy in the United States (total of 81% in 2016) [1]. To meet the expanding demand for petroleum and natural gas, great attention has been given to the development of unconventional oil and gas reservoirs. Generally, unconventional reservoirs can be categorized into the tight and shale reservoirs, coalbed methane reservoirs, gas hydrates, heavy oil, and tar sands, among others. Shale reservoirs worldwide are associated with high total organic carbon (TOC), with an estimated reserve that is equivalent to 345 billion barrels of oil and 7299 trillion cubic feet of gas [2]. Based on the initial fluid properties and phases at the reservoir condition, as well as the phase behavior changes during the production process, shale reservoirs are grouped into three categories: shale oil reservoirs, shale gas reservoirs, and shale

gas-condensate reservoirs. However, until recently, it was challenging to unlock shale oil or gas because of the extremely small pore size, low porosity, and ultra-low permeability of shale. Over the last decade, two advanced technologies—horizontal drilling and multistage hydraulic fracturing—have been successfully applied in shales and made it profitable to boost oil or gas production from such tight formations. In 2015, oil and gas production from unconventional shale oil and gas plays was 4.89 million barrels per day and 37.4 billion cubic feet per day, respectively, which accounted for approximately half of the total U.S. crude oil and natural gas production [3]. By using intensive horizontal drilling and hydraulic fracturing techniques, oil or gas escapes from the tight matrix to the hydraulic fractures through primary depletion under the reservoir depressurization or by gas expansion drives, boosting a tremendous increase in production. Nevertheless, field production data invariably indicated, after a few years of production, a sharp decline in oil or gas production rate was observed, followed by a prolonged low-production rate period. Only less than 10% of oil was recovered from the unconventional formations during this primary depletion period [4], resulting in an enormous unrecovered oil bank remaining in the reservoir.

Recently, gas injection enhanced shale oil/gas recovery methods, including huff-n-puff gas injection (or cyclic gas injection) and gas flooding, have been experimentally studied at the laboratory scale or conducted in field, and numerically examined through simulation by many researchers [5–17]. Generally, the injected gas could be carbon dioxide, nitrogen, flue gases ($N_2 + CO_2$), and produced gas, depending on shale fluids with unique characteristics at specific reservoir conditions. Injected CO_2 in shale reservoirs not only could be permanently sequestered within the small pores in an adsorbed state, but also could participate in enhancing recovery of oil or natural gas through maintaining pressure, multi-contact miscible displacement [10,11], molecular diffusion [13,16,18], or desorption of methane [13,18–20]. N_2, as an economic and eco-friendly alternative, could displace oil mostly through an immiscible displacement approach because of the high minimum miscibility pressure (MMP). Owing to the low viscosity of N_2, viscous fingering may occur during the displacement process. Flue gas, as the mixture of CO_2 and N_2, is also deemed as a potential injection gas resource for shale reservoirs and has been successfully injected in other unconventional reservoirs (coalbed methane and gas hydrate); however, not so many research studies have been carried out yet regarding flue gas injection in shale reservoirs. Moreover, substantial produced gas associated with oil production is flared or vented into the air during oil recovery, which is not only energy waste, but also hazardous to the environment [21–23]. In order to reduce gas flaring or venting and compensate for the oil production decline, produced gas could be effectively used for recycled gas enhanced oil recovery (EOR).

This paper aims to offer a holistic guideline about the feasibility and advances of gas injection in shale reservoirs, including shale oil, gas, and condensate reservoirs. The gas injection techniques for different unconventional reservoirs are investigated. Finally, CO_2 sequestration and gas injection and utilization in unconventional reservoirs as an alternative for flaring or venting are reviewed and discussed.

2. Shale Oil Reservoirs

Driven by the two key techniques of horizontal drilling and intensive hydraulic fracturing application, U.S. shale reservoirs have boosted oil production significantly since 2010 from the prolific shale plays, such as Bakken, Eagle Ford, and Permian. In 2013, the technically-recoverable shale oil resources were estimated at 345 billion barrels, which accounted for 10% of the total crude oil in the world [24]. Among the top countries with identified shale oil resources, United States, with an estimated reserve of 58 billion barrels, ranked second, while Russia, with 75 billion barrels, ranked first. China, Argentina, and Libya with estimated reserves of 32, 27, and 26 billion barrels, respectively, ranked third to fifth among the largest shale oil resources [24]. The technically-recoverable shale oil resources in eight regions of the world are shown in Figure 1 [25]. In 2015, tight oil production reached 4.89 million barrels per day, which accounted for half of the total U.S. crude oil production [3]. Bakken, Eagle Ford, and Permian, as the three largest oil shale reservoirs, contribute to 75% of the total annual

unconventional oil production in the U.S. In addition to the above mentioned three remarkable shale plays, other important shale oil formations, such as the Niobrara Shale, Anadarko–Woodford, and Marcellus have also made great contributions to unconventional crude oil production. It is predicted from the Annual Energy Outlook 2017 (AEO 2017) reference case that shale oil production would take up the most of U.S. crude oil production in 2020 with an increasing rate of 6 million barrels per day [26].
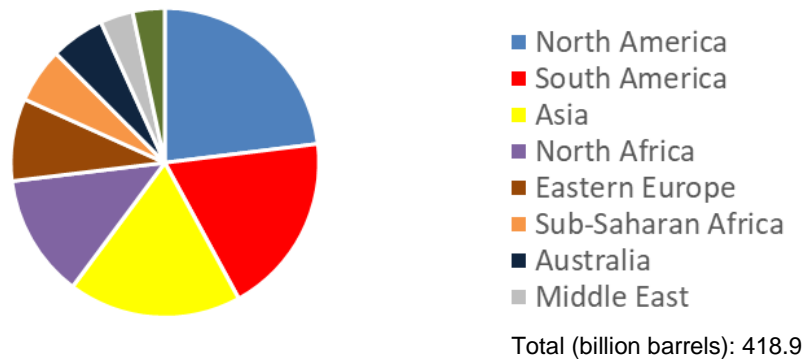

■ North America
■ South America
■ Asia
■ North Africa
■ Eastern Europe
■ Sub-Saharan Africa
■ Australia
■ Middle East

Total (billion barrels): 418.9

Figure 1. Technically-recoverable shale oil in eight different regions by 2015. Reproduced from [25], 2015, Energy Information Administration (EIA).

2.1. Enhanced Oil Recovery Methods

Injecting fluid into extra-low permeability shale reservoirs faces the severe issues of early breakthrough times and poor sweep efficiencies. Water floods, commonly being used in conventional reservoirs as an improved oil recovery (IOR) method, has been proven to be unfeasible in tight unconventional shale formations [17,27]. In the past decade, gas injection, including huff-n-puff injection or cyclic gas injection, and gas flooding, has been demonstrated to be a promising EOR method for shale reservoirs and has been extensively studied in oil and gas research laboratories and widely modeled through numerical simulation methods by many researchers [8–12,14,16,17]. We review the recent research progress on gas injection in shale oil reservoirs through huff-n-puff (Section 2.1.1) and gas flooding (Section 2.1.2) methods and summarize the gas injection mechanisms in Section 2.1.3. We also describe the current state of field pilots of gas-injection for EOR, in Section 2.1.4, based on the available reported and published resources. The experimental and simulation studies on different gas injection approaches for shale EOR are summarized in Tables 1 and 2. Table 1 summarizes the laboratory-measured oil recovery factors (in terms of initial saturated oil/OOIP) by adopting various gas injection schemes using different shale rocks (permeability ranges 10^2 nd to 10^{-1} md). Table 2 highlights the increased oil recovery factor by applying different gas injection schemes compared to the primary depletion scheme.

2.1.1. Huff-N-Puff Gas Injection Performance Evaluation

The experimental study of huff-n-puff gas injection or cyclic gas injection in tight rock samples have been conducted in multiple publications [9,11,28]. The schematic diagram of an experimental setup for gas flooding and huff-n-puff gas injection is shown in Figure 2. In Brief, the first step is to saturate core plugs with oil samples at a given pressure for a reasonably long time. Then, the pre-saturated cores are placed in a core holder and exposed to high-pressure gas. During a shut-in or soaking period, the gas is expected to penetrate into the matrix and make sufficient contact with oil. After the soaking period, the oil is seeping out from the matrix through decreasing the pressure in the system. The oil recovery is calculated by re-weighting the core sample or through collecting the recovered oil using organic solvents. The commonly used injection gases or solvents are N_2, CO_2, CH_4, C_2H_6, and CH_4/C_2H_6 mixture. The core plug samples were mostly selected from Eagle Ford [9,28], Bakken [10,11,29,30], and Barnett and Marcos [31]. As shown in Table 1, Middle Bakken has a relatively large permeability [10,29,30] compared to other shales.
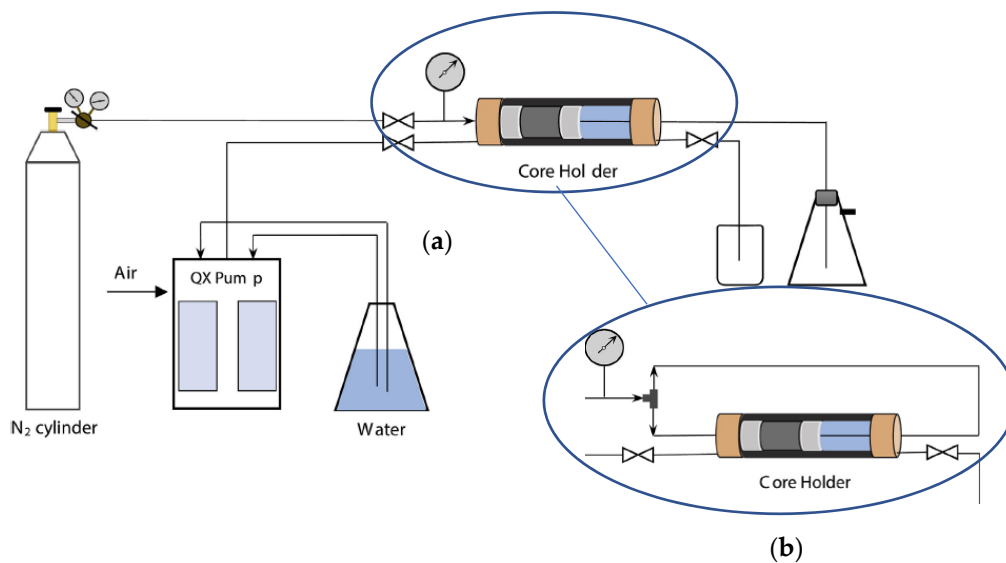
Figure 2. Schematic diagram of experimental setup for (**a**) gas flooding and (**b**) huff-n-puff gas injection. Reprint with permission [9], 2017, Elsevier.

Sensitivity Analysis

In addition to experimental studies, a number of simulation work has been performed using in-house simulation approaches or commercial software tools to study field-scale huff-n-puff injection in tight formation. Sensitivity analysis is conducted along with experiments or simulations to examine effects of various operation parameters (injection pressure and rate, initial injection time, gas injection duration, soaking time, number of cycles, and heterogeneity) on recovery performance and will be discussed in the following section.

The effect of gas injection pressure on oil recovery in the huff-n-puff scheme has been investigated in many literature works. A general conclusion was that recovery factor was increased with increasing injection pressure. Some authors concluded that re-pressurization is the primary oil recovery mechanism for the huff-n-puff process [7,31,32]. Further investigations [29,32] indicated that increasing pressure only resulted in a good recovery performance at immiscible condition. When the injection pressure was above the MMP, a further increase in injection pressure could not result in a significant increase in recovery factor. The experimental results from one study [29] showed that near-miscible and miscible CO_2 huff-n-puff injection could effectively enhance crude oil recovery up to 63.0% and 61.0% respectively, while water flooding and immiscible CO_2 huff-n-puff would result in final recovery factor of 42.8% and 51.5%, respectively. They concluded that dominant mechanisms for the huff-n-puff process in shale oil formations included viscosity and interfacial tension reduction, oil swelling effect, light-components extraction, and solution gas drive. It should be noted that the Bakken rock samples used in their study is not ultra-tight, but tight (permeability in 10^{-1} md). This conclusion may well explain the mechanisms of huff-n-puff in conventional or tight formation, where gas is comparatively easier to dissolve into the matrix; but further analysis may be required to better understand the mechanisms of huff-n-puff gas injection in ultra-tight formation, where oil is trapped in nanosized pores and gas is more difficult to get in contact with oil. Recently, one study [33] used CT scanning technology to monitor the saturation change with time in an organic-rich Eagle Ford core plug. The core sample was placed in a high-pressure CO_2 core holder, below and above MMP, and they observed that when injection pressure was above MMP, the recovery was still increasing with increasing pressure.

Gas injection rate is one of the most important parameters in huff-n-puff gas injection EOR. Yu et al. [34] conducted a series of sensitivity analysis and concluded that gas injection rate was the most important parameter to enhance oil recovery in comparison to other factors, such as injection time and number of cycles. It was also concluded that a higher injection rate resulted in a higher oil

recovery factor [15,34,35]. Other studies examined the effect of CO_2 injection rate on oil recovery factor by using the injection rate of 500 and 5000 Mscf/day [15] and 100, 1000, and 10,000 Mscf/day [35], and found out that the recovery factor was increased by 1.0–5.4%, correspondingly. The result is not a total surprise as higher injection rates ensure more gas to be injected into the reservoir in one cycle, keeping the reservoir pressure high. On the other hand, higher injection rate also means more capital investment, especially when the injection rate is increased by one or two orders, much more CO_2 would be injected into the reservoir. From a profitability standpoint, it is not reasonable to inject a large amount of CO_2, and economic evaluation should be conducted to optimize the injection rate.

The initial gas injection time and injection duration are also two key parameters in gas injection process. Sun et al. [15] found delaying the initial gas injection time from 1000 days to 2000 days could increase the oil recovery by 2.47%. Sanchez-Rivera et al. [14] investigated the initial gas injection time by adopting 30, 200, 400, 500, and 1000 days of primary depletion. They also concluded that delaying the start of huff-n-puff injection (from 30 to 400 days) yielded an increased recovery; however, when the gas injection was started at a later time (400 to 1000 days) oil recovery was not enhanced effectively. Similar to cycle numbers and gas injection rate, longer gas injection time is beneficial to oil recovery because larger volume of gas would be injected into the formation and maintain a high reservoir pressure. However, from a cash-flow perspective, gas injection duration should be optimized.

Soaking time, as another important operation parameter in the huff-n-puff process, is normally examined along with cycle numbers. Long soaking time enabled the injection gas to better mix with oil through dissolution, thereby improving the efficient recovery per mole of CO_2. However, a long shut-in period would result in a shorter production time. The optimum soaking time can be determined by calculating the gross/net gas utilization [7], as well as associating the cycle numbers and pressure distribution [36]. Some experimental and simulation results indicated that at miscible CO_2 injection condition, a longer soaking period allowed gas to diffuse further into the matrix, leading to a higher accumulative recovery [7,31,32]. Some studies reported that in a fixed duration of time, shortening the soaking time and allowing for more cycle numbers was more effective than a long soaking time with fewer cycles [9,15,32,37]. Chen et al. [5] realized that the cumulative recovery after a certain period of time for CO_2 huff-n-puff injection was lower than that of the primary depletion. They explained that for the huff-n-puff process, the injection and soaking periods resulted in a shorter production time and caused uncompensated production loss. Sheng [27] used an in-house model to repeat the case and verified the simulation results. The author explained that the low final recovery factor for huff-n-puff injection in the former publication was a result of the low injection pressure of 4000 psi, which should have been higher than the initial reservoir pressure of 6840 psi. In another study by Sun et al. [15], it was concluded that soaking time (1, 15, 100 days) had zero effect on the recovery performance. It is worth noting that, in this sensitivity analysis, only one cycle of gas injection was performed after 1000 days of primary depletion while the total production time was 5000 days and the soaking period was far shorter compared to the production time.

The effect of heterogeneity of reservoir formation on huff-n-puff or cyclic natural gas injection efficiency has also been investigated [5,7,16,37]. The common conclusion that was drawn by different authors was that the recovery factor for a heterogeneous reservoir with low-permeability region outperformed homogenous reservoirs, since, for the latter one, CO_2 migrates into the deeper formation without playing the role of increasing the reservoir pressure and carrying oil back to the well. Reservoir heterogeneity could effectively prevent injected gas moving to the deeper formation and contribute to maintaining a relatively-high near-well reservoir pressure.

In addition to the above mentioned sensitivity analysis study, the effect of molecular diffusion and nanopore confinement effect on recovery during huff-n-puff gas injection in tight formation were addressed in some studies.

Generally, two different empirical correlations found by Sigmund [38,39] and Wilke and Chang [40] are used to estimate the diffusion coefficients in bulk phase and also have been incorporated in

commercial software tools (GEM, CMG). In Sigmund correlation, the binary diffusion coefficient, D_{ij}, between component i and j, is calculated by:

$$D_{ij} = \frac{\rho_k^0 D_{ij}^0}{\rho_k}\left(0.99589 + 0.096016\rho_{kr} - 0.22035\rho_{kr}^2 + 0.032874\rho_{kr}^3\right) \tag{1}$$

where $\rho_k^0 D_{ij}^0$ is the zero pressure limit of the density-diffusion coefficient product in phase k; and ρ_k and ρ_{kr} are the molar density and reduced molar density of the diffusion mixture, respectively.

$$\rho_k^0 D_{ij}^0 = \frac{0.0018583 T^{1/2}}{\sigma_{ij}^2 \Omega_{ij} R}\left(\frac{1}{M_i} + \frac{1}{M_j}\right)^{1/2} \tag{2}$$

$$\rho_{kr} = \rho_k \frac{\sum_{i=1}^{n_c} y_{ik} v_{ci}^{5/3}}{\sum_{i=1}^{n_c} y_{ik} v_{ci}^{2/3}} \tag{3}$$

M_i is the molecular weight of component i; σ_{ij} is the collision diameter; Ω_{ij} is the collision integral of the Lennard-Jones potential; y_{ik} is the mole fraction of component i in phase k; and v_{ci} is the critical volume of component i. σ_{ij} and Ω_{ij} are calculated by:

$$\sigma_{ij} = \frac{\sigma_i + \sigma_j}{2} \tag{4}$$

$$\sigma_i = (2.3551 - 0.087\omega_i)\left(\frac{T_{ci}}{P_{ci}}\right)^{1/3}$$

$$\Omega_{ij} = \frac{1.06036}{T_{ij}^{0.1561}} + \frac{0.193}{\exp(0.47635 T_{ij})} + \frac{1.03587}{\exp(1.52996 T_{ij})} + \frac{1.7674}{\exp(3.89411 T_{ij})} \tag{5}$$

where ω is acentric factor; T_{ci} is the critical temperature; and P_{ci} is the critical pressure. The diffusion coefficient of component i in a multicomponent mixture of phase k is calculated as:

$$D_{ik} = \frac{1 - y_{ik}}{\sum_{i \neq j} \frac{y_{jk}}{D_{ij}}} \tag{6}$$

In Wilke–Chang correlation [40], the diffusion coefficient was determined based on a series of laboratory measurements for various hydrocarbon solvents and other systems in the literature, and is expressed by:

$$D_{ik} = \frac{7.4 \times 10^{-8}(M_{ik}')^{1/2} T}{\mu_k v_{bi}^{0.6}} \tag{7}$$

$$M_{ik}' = \frac{\sum_{j \neq i} y_{jk} M_j}{1 - y_{ik}} \tag{8}$$

where M_{ik}' is the molecular weight of solvent; μ_k is the viscosity of phase k; and v_{bi} is the partial molar volume of component i at the boiling point. It should be noted that Wilke–Chang (1955) correlation was developed for low-pressure liquid systems and a recent study indicated that the application of Wilke–Chang correlation is not suitable for high-pressure shale fluids [41].

A more generalized diffusion correlation was developed by Leahy-Dios and Firoozabadi (2007), which is capable of estimating the diffusivities of gas, liquid, and supercritical states of nonpolar binary or multicomponent mixtures at a wide pressure and temperature range [42]. The Leahy-Dios and Firoozabadi correlation is expressed as:

$$\frac{cD_{21}^{\infty}}{(cD)^0} = A_0 \left(\frac{T_{r,1}P_{r,2}}{T_{r,2}P_{r,1}}\right)^{A_1} \left(\frac{\mu}{\mu^0}\right)^{[A_2(\omega_1,\omega_2)+A_3(P_r,T_r)]} \tag{9}$$

Where c is the molar density (mol/m^3) of component 1; μ is the viscosity (Pa·s) of component 1; and $(cD)^0$ and μ^0 are the dilute gas density-diffusion coefficient product (mol/m·s) and viscosity (Pa·s), respectively. $T_{r,i}$ and $P_{r,i}$ are the reduced pressure and temperature ($T/T_{c,i}$ and $P/P_{c,i}$). The constants A_0 to A_3 are calculated as follows:

$$A_0 = e^{a_1} \tag{10}$$

$$A_1 = 10a_2 \tag{11}$$

$$A_2 = a_3(1 + 10\omega_1 - \omega_2 + 10\omega_1\omega_2) \tag{12}$$

$$A_3 = a_4\left(P_{r,1}^{3a_5} - 6P_{r,2}^{a_5} + 6T_{r,1}^{10a_6}\right) + a_7 T_{r,2}^{-a_6} + a_2\left(\frac{T_{r,1}P_{r,2}}{T_{r,2}P_{r,1}}\right) \tag{13}$$

where $a_1 = -0.0472$ $a_2 = 0.0103$ $a_3 = -0.0147$ $a_4 = -0.0053$ $a_5 = 0.3370$ $a_6 = -0.1852$ $a_7 = -0.1914$.

Extensive measurements have been performed to estimate the diffusion coefficient of a solute in a bulk phase. However, there are limited experimental data in the literature about measurement of diffusion coefficient within a porous solid. An effective diffusion coefficient (D_{eff}) is suggested by combining the tortuosity factor of a matrix (τ) and/or porosity (ϕ) with the bulk diffusion coefficient (D) to characterize the diffusion behavior in a porous media. Some researchers [43–45] related the D_{eff}/D to porosity and tortuosity factor by the following expression:

$$\frac{D_{eff}}{D} = \frac{\phi}{\tau} \tag{14}$$

In some studies [46,47], D_{eff}/D is expressed as:

$$\frac{D_{eff}}{D} = \phi^{m-1} \tag{15}$$

where m is the shape factor, which is in the range of 1.3–2 for sands and sandstones and in the range of 1.87–3.28 for clay [48].

Yu et al. [16] built a compositional simulation model to examine the effect of molecular diffusion in CO_2 huff-n-puff injection in Bakken formation (10 μD) using three different CO_2 diffusion coefficients (10^{-2}, 10^{-3}, and 10^{-4} cm^2/s). The molecular diffusion term and mechanical dispersion term were incorporated in the dispersivity coefficient, which is expressed by:

$$\overline{\overline{K}}_{ik} = \frac{\overline{\overline{D}}_{ik}}{\tau} + \frac{\overline{\alpha}_k|\overline{u}_k|}{\phi S_k} \tag{16}$$

where $\overline{\overline{K}}_{ik}$ is the dispersivity coefficient of component i in the phase k; $\overline{\alpha}_k$ is the dispersivity of phase k in the three directions; u_k is the Darcy's flow velocity; and S_k is the saturation of phase k. D_{ik} is calculated by using Sigmund correlation [38,39]. After three years of primary production, CO_2 was injected through a horizontal well with an injection rate of 500 Mscf/day (1 year injection +3 month shut-in). Compared to the primary depletion, the oil production at 30 years was increased by 3.25%, 1.40%, and 0.10% for diffusion coefficients of 10^{-2}, 10^{-3}, and 10^{-4} cm^2/s, respectively. They concluded that diffusion was an important mechanism in the CO_2 huff-n-puff process in tight formations. However, it should be noted that the CO_2 diffusion coefficients applied in this study were larger than the experimental data, which is in the order of 10^{-5} cm^2/s. Moreover, without including molecular diffusion (equivalent to an extremely small diffusion coefficient) in CO_2 huff-n-puff gas injection, the oil recovery factor was reduced by around 2% compared to primary depletion. Therefore, it is worthwhile to conduct a sensitive analysis to examine the effect of molecular diffusion on recovery performance using a

smaller diffusion coefficient of 10^{-5} cm^2/s. Zhang et al. [35] used the same simulation model to examine the effect of molecular diffusion and nanopore confinement on the huff-n-puff injection process at a field-scale. They successively compared Cases B (CO_2 injection with CO_2 molecular diffusion), C (CO_2 injection with capillary pressure), and D (CO_2 injection with CO_2 molecular diffusion and capillary pressure) to Case A (without CO_2 injection) to investigate the effects of CO_2 molecular diffusion and capillary pressure on the CO_2 huff-n-puff process. Nevertheless, this design faces a serious issue. Case A is a primary depletion process without CO_2 injection. The incremental oil recovery of 2.8% in Case B compared to Case A may be owing to the integrated mechanisms of gas injection, rather than CO_2 molecular diffusion only. Similarly, it is improper to conclude that the capillary pressure effect played a critical role based on the comparison of Case C to A. It is suggested that instead of taking Case A as the base case, they come up with a new base case (a Case E): CO_2 injection without considering these two effects, and compare the well performance of Cases B, C, and D to Case E. Sun et al. [15] investigated the CO_2 huff-n-puff in unconventional liquid reservoirs with complex fracture networks and concluded that the effect of diffusion is negligible in the huff-n-puff process. However, the duration of huff-n-puff (30 day injection + 15 day shut-in) was too short compared to the total production time (5000 day); after the soaking period, the injected CO_2 would flow back to the surface instead of diffusing into the matrix and mixing with oil sufficiently. In addition, CO_2 diffusion coefficients in this study were in the range of 10^{-7}–10^{-9} cm^2/s, which were much smaller than those in the previous study [16]. Using smaller diffusion coefficients was probably another reason to explain the negligible diffusion effect in the huff-n-puff process. Alfarge et al. [49] found that molecular diffusion played a positive role in huff-n-puff process but had a negative effect in flooding scheme.

Multiple phase behavior research studies have been conducted recently investigating the gas injection characteristics of oil shale reservoirs influenced by confinement effect in nanopores. Teklu et al. [50] used the multiple mixing cell method (MMC) to calculate MMP of Bakken oil during injection of CO_2 and mixtures of CO_2 and CH_4 while critical pressure and temperature of the fluids were shifted due to confinement effects. They recognized MMP reduction of 600 psi due to the shift in critical properties; however, they concluded that the large gas–oil capillary pressure owing to nanopores did not influence MMPs. Zhang et al. [51] used method of characteristics (MOC), multiple mixing cells, and slim tube simulation approaches to examine capillary pressure effect on MMP. For CO_2 injection, inclusion of high capillary pressure would enhance the recovery of heavy oil components for around 10% in the immiscible pressure region. In addition, capillarity effect might change the MMP and this change varied for different fluid compositions. For a ternary mixture, this influence would decrease MMP; for the Bakken fluid, MMP increased with high capillary pressure, and for the Eagle Ford fluid, no significant change of MMP was observed. In a similar study, Zhang et al. [52] calculated MMPs for CO_2 floods in Bakken and concluded that the MMP was reduced by 5% due to the confinement effects of nanopores, including both large capillary pressures and the shift in critical properties. It should be noted that in this study and another similar study [10], the MMP was measured by using the vanishing interfacial tension (VIT) method, which has been shown to have significant limitations even for conventional reservoirs [53]. Nojabaei and Johns [54] studied the effect of large gas–oil capillary pressure on fluid properties and saturation pressures when the produced gas was injected to enhance oil recovery. They showed that as the original oil mixed with the injection gas, the effect of capillary pressure on recoveries would get smaller. They did not recognize any change in the MMP of produced gas with the original oil due to large gas–oil capillary pressure. One reason for not recognizing a change in MMP can be that they used a compositionally-extended black oil approach with two oil and gas pseudo-components. The MMP would be the same as the critical point of this pseudo-binary mixture, at which interfacial tension (IFT), and subsequently gas–oil capillary pressure would be zero. Wang et al. [55] developed a Parachor model to account for the effect of confinement on interfacial tensions (IFTs). They used their model to calculate CO_2 MMP of Bakken oil. They concluded that for the pores larger than 10 nm, MMP is independent of pore width. For a pore width of 3 nm, they observed 67.5% and 23.5% decrease in IFT and MMP, respectively. Huang et al. [56] proposed that

including capillary pressure effect could reduce oil and gas recovery, meanwhile, alter the compositions of residuals. Du et al. [57] used a black-oil simulation approach to examine the capillary pressure effect in the huff-n-puff gas injection process in a tight formation. Inclusion of the capillary pressure effect in phase behavior could increase the oil recovery at a lower production pressure. However, at miscible or near-miscible conditions, the influence of capillary pressure on reservoir performance was decreased owing to the reduced IFT between oil and gas phases.

2.1.2. Gas Flooding Performance Evaluation

In the literature, experimental and simulation studies of gas flooding in shale reservoirs are limited compared to huff-n-puff, probably owing to the low injectivity of tight shale rock. Yu et al. [9] experimentally compared N_2 flooding to N_2 huff-n-puff by using Eagle Ford shale core plugs (with permeability of 85–400 nd). In the gas flooding scheme, the production rate was decreased after N_2 breakthrough. The huff-n-puff production scheme maintained a relatively longer effective recovery performance owing to the continuous favorable pressure gradient in each cycle. It should be noted that the experimental conditions (P_{inj} = 1000 psia, T = 72 °F) failed to reflect the real reservoir pressure and temperature. Yang et al. [30] experimentally examined the CO_2 WAG (water-alternating-gas) injection in tight Bakken formation cores (with permeability of 250–440 µd) at reservoir temperature of 140 °F. The results indicated that shorter water slug size or a longer CO_2 slug size was beneficial for improving fluid injectivity, but resulted in a decrease in recovery efficiency because of early gas breakthrough. Similarly, an increase in cycle time during water injection period led to a decrease in the fluid injectivity. However, after the fluid injectivity was decreased to a threshold value, it became sensitive to CO_2 slug size instead.

Among the simulation studies, Sheng and Chen [17] evaluated and compared natural gas injection and water injection methods in hydraulically-fractured shale oil reservoirs (with permeability of 0.1 µd). A small model was used to simulate gas flooding between two lateral hydraulic fractures of a horizontal well. They concluded that the gas flooding method resulted in a slightly higher oil recovery than cyclic gas injection method; however, the former required a much greater amount of injection gas than the latter. Water injection performance was not as good as gas injection because of the low water injectivity in the shale reservoir. Hoffman [8] performed a numerical simulation model to examine gas flooding at both miscible and immiscible conditions in shale oil reservoirs at the Elm Coulee Field. The results indicated that significant oil recovery could be achieved regardless of injection gas types at both miscible and immiscible conditions. Hydrocarbon gas as an alternative injection gas performed as well as CO_2 injection at miscible condition. At immiscible condition, hydrocarbon injection could also result in favorable recovery.

Table 1. The experimental studies about different gas injection approaches in shale reservoirs for EOR.

Oil Sample	Rock Sample	K (μd)	Porosity (%)	Injection Gas	Method	Pinj (psi)	T (°F)	Production	Oil RF (%)	Reference
		Experimental Study								
Dead oil from Wolfcamp shale	Eagle Ford	0.085	4.4	N_2	flooding	1000	72	48 h	17.94	[9]
					huff-n-puff				22.52	
		0.4	13.1		flooding				19.88	
					huff-n-puff				24.13	
Mineral oil (Soltrol-130)	Eagle Ford	0.5	5	N_2	cyclic gas injection	1000	95	-	14.23–45.45	[28]
									11.41–39.66	
C_{10}-C_{13} Isoalkanes	Eagle Ford	-	7.7	CO_2	cyclic gas injection	850–3500	95	-	20-71	[7]
	Mancos	-	5			850–500			10–31	
						3500			43–63	
Bakken oil	Middle Bakken	8.1–103.5	4.4–5.4	C_1	oil extraction	5000	230	24 h	>90	[10]
				C_2					nearly 100	
				C_1/C_2 (85/15)					>90	
				CO_2					>90	
				N_2					26	
	Lower Bakken	5.25	3.8	C_1					≈18	
				C_1/C_2 (85/15)					≈27	
				CO_2					≈32	
				N_2					<10	
Bakken oil	Upper Bakken	-	-	SC CO_2	oil extraction	5000	230	7 h	≈10–43	[11]
	Lower Bakken	-	-						≈8–48	

Table 1. *Cont.*

					Experimental Study					
Oil Sample	Rock Sample	K (μd)	Porosity (%)	Injection Gas	Method	Pinj (psi)	T (°F)	Production	Oil RF (%)	Reference
Mineral oil (Soltrol-130)	Barnett	-	-	N_2	cyclic gas injection	1000	95	1 d (soaking)	6.5	[31]
						2000			11.23	
						3000			14.91	
						3500			17.79	
	Marcos	-	-			3000		1 d (soaking)	13.5	
								2 d (soaking)	16.96	
								3 d (soaking)	19.59	
Bakken oil	Bakken	270–830	18.6–23.1	CO_2	near-miscible huff-n-puff	1349	140	40 h	63	[29]
					miscible huff-n-puff	2031		60 h	61	
					waterflodding	1668		-	51.5	
					immiscible huff-n-puff	1015		60 h	42.8	
Bakken oil	Bakken	290–440	18.9–23.6	water+CO_2	water-alternating-CO_2-		145.4	-	80.1–88.1	[30]
Wolfcamp	Eagle Ford	0.24	7.28	CO_2	huff-n-puff	1600	72	7 h (soaking)	56.8 (7 circles)	[58]

Table 2. The simulation studies about different gas injection approaches in shale reservoirs for EOR.

Simulation Study											
Formation	**K (µD)**	**ϕ (%)**	**Injection**	**Method**	**Natural Fracture**	**Model**	**Diffusion**	**Confiment Effect**	**Production**	**Increased Oil RF (%)**	**Reference**
Field-scale	0.1	6	CO_2	huff-n-puff	30 mD	DFN	Yes	Yes	5000 d	10 (0.1 uD) 131.8 (1 uD) 11.5 (inject for 60 d) 13.3 (inject for 200 d)	[15]
Bakken	1 10 100	7	CO_2	huff-n-puff	NA	Single porosity	Yes	No	30 y	2.35 1.4 −0.7	[16]
Bakken	10, 0.001	8	CO_2	huff-n-puff	NA	Single porosity	No	No	60 d	≈−0.6–0.01	[37]
Bakken	10 (homo01) 10 (hete04)	8	CO_2	huff-n-puff	NA	Single porosity	No	No	700 d	−0.13 (10 d soaking) −0.23 (20 d soaking) −0.24 (10 d soaking) −0.33 (20 d soaking)	[5]
Bakken	10	8	CO_2	huff-n-puff	NA	Single porosity	Yes	No	5500 d	10.9 (Ppro = 1000 psia, 3 circles) 22.8 (Ppro = 2900 psia, 3 circles) 16.5 (Ppro = 3500 psia, 3 circles) ≈0 (inject after 30 d, 1 circle) 0.6 (inject after 200 d, 1 circle) 0.9 (inject after 500 d, 1 circle)	[14]
Eagle Ford	0.1	6	CO_2	gas flooding cyclic gas injection waterflooding cyclic waterflooding	NA	Single porosity	No	No	70 y	15.12 14.42 11.9 11.03	[17]
Middle Bakken	50	10	produced gas	huff-n-puff	NA	Single porosity	No	Yes	800 d	15.4 (Pinj = 1000 psi)	[57]
Middle Bakken	1 100	7	CO_2	huff-n-puff gas flooding huff-n-puff gas flooding	Conductivity 30 mD-ft	EDFM	Yes	No	18 y	2.56 −1.79 14.34 30.06	[59]
Middle Bakken	20	5.6	CO2	huff-n-puff	NA	EDFM	Yes	No	7000 d	5.9 (3 cycles)	[60]
Bakken	1	8	CO2	huff-n-puff	1.2 mD 4 mD	Dual permeability	Yes	No	>7000 d	55.1 49.8	[61]
Eagle Ford	0.9	12	CO2	huff-n-puff	Conductivity 10 mD-ft	EDFM	Yes	Yes	7300 d	9.1 (D = 0.01 cm^2/s) 3.8 (D = 0.001 cm^2/s) −5.1 (D = 0.0001 cm^2/s) −6.9 (D = 0.00001 cm^2/s)	[62]

2.1.3. Gas Injection Mechanisms

For huff-n-puff gas injection in shale oil reservoirs, re-pressurization is one of the most important mechanisms for EOR and could be achieved by using high injection pressure [29,31,33], by increasing the injection rate [15,34], by extending the injection duration, and by increasing the cycle numbers [32,37]. It is necessary to optimize these operational parameters of a huff-n-puff injection process from profit-motive and cash flow perspectives. Another important mechanism is that the injected solvents (CO_2, CH_4, C_2H_6, or produced gas) could extract the light components from the oil through a multi-contact miscible process. Meanwhile, those solvents dissolve into the oil, leading to a viscosity and interfacial tension reduction and the swollen-diluted oil is much easier to be recovered. The above mentioned mechanisms may play important roles in tight (e.g., Middle Bakken formation) or conventional reservoirs, where gas is relatively easier to diffuse into the matrix and to make contact with oil. Recent studies visualized the gas sweep volume in ultra-tight shale plugs by using CT images [33,58], indicating that gas could make contact with the oil that is trapped in nanosized pores. Furthermore, the nanoconfinement effect may influence the estimations of MMP and alter the fluid properties, so the inclusion of capillary pressure effect and the shift in critical properties results in more accurate recovery prediction [52,54]. In addition, the mechanism of molecular diffusion in shale reservoirs is controversial in the literature. The effect of molecular diffusion on recovery performance is highly related to the diffusion coefficient and soaking time. Nevertheless, laboratory measurements of gas diffusion coefficient in oil-saturated tight porous media is limited. A more reliable diffusivity is crucial for accurately evaluating the role of molecular diffusion in huff-n-puff gas injection. The effect of matrix permeability on EOR is also evaluated by plotting the increased oil recovery factor versus matrix permeability in Figure 3. Different colors represent different simulation works in Table 2. Huff-n-puff shows a promising performance on EOR at a wide range of permeability. The various results attribute to the variety of simulation models with different incorporations of effects. Generally, a dual porosity dual permeability system with developed natural fractures [59–62], that included nanoconfinement effect, and molecular diffusion by employing a higher diffusivity, and adopted optimized huff-n-puff parameters (cycles, injection time, etc.), could achieve a better recovery performance.
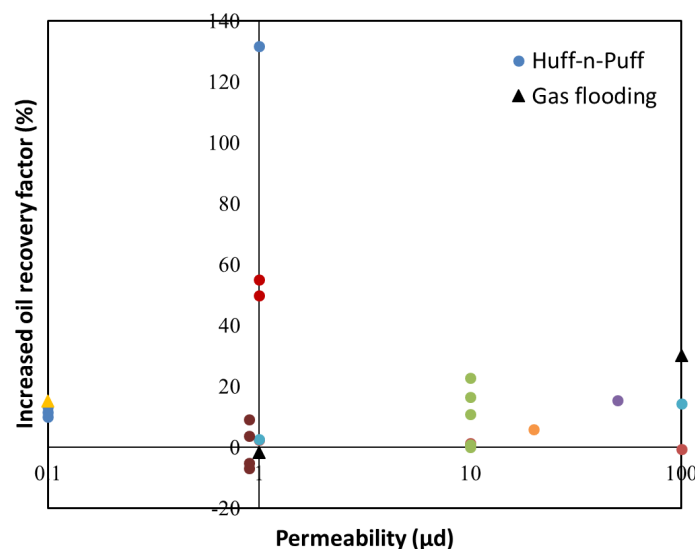

Figure 3. Incremental oil recovery factor of huff-n-puff and gas flooding from simulation studies (Table 2), for the range of matrix permeability from 0.1 to 100 μd. Different colors represent different simulation studies.

In the ultra-tight shale matrix, gas flooding was less effective compared to huff-n-puff gas injection in shale reservoirs because of the low gas injectivity. It would take a much longer time for the injection gas to migrate from the injection well to the production well. A closed pair of injection and production

wells (e.g., 200 ft apart in [17]) and highly developed natural fractures or effective hydraulic fractures could alleviate this issue to some extent. At relatively high-permeability shales, the performance of gas flooding is improved and surpasses huff-n-puff over a turning point of permeability, as shown in Figure 4 [59]. In addition, solvent (CO_2, CH_4, or produced gas) flooding still outperformed pure water flooding in tight (and not ultra-tight) formations, since solvent could be miscible with oil, reduce oil viscosity, and lead to a larger volume of contacted oil compared to water. CO_2 WAG injection, as an alternative for EOR in tight formations, combines the advantages of water flooding and CO_2 continuous flooding, leading to an improved macroscopic sweeping efficiency and an enhanced microscopic displacement efficiency.
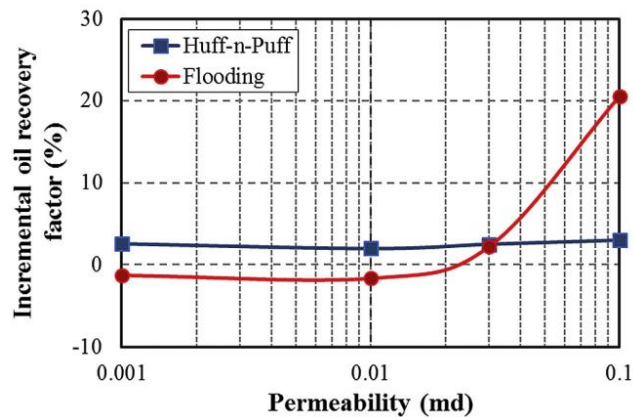

Figure 4. Comparison of incremental oil recovery factor between CO_2 flooding and CO_2 huff-n-puff, for the range of permeability from 0.001 to 0.1 md Reprint with permission [59], 2017, Elsevier.

2.1.4. Field Pilots

Even though experimental core flooding tests and simulation results imply great potential of gas injection EOR in shale formation, the oil and gas industry still remains in the field trial stage. Many oil companies have devoted field pilots for gas injection EOR in oil-rich shale reservoirs. So far, some reported field pilots in Bakken formation are not successful, but a number of field pilots in the Eagle Ford showed encouraging performance. EOG Resources have focused on field pilots of gas injection EOR in both Bakken and Eagle Ford shale plays since 2013 [63]. EOG is the first company that disclosed seeing a significant increase (30% to 70%) in oil production in Eagle Ford through gas injection. They indicated that key factors to enhance the gas injection EOR effectiveness include stimulating the most productive rock and effectively fracturing. However, field pilots in Bakken were unsatisfactory because it was difficult for the gas to penetrate the tight formation. EERC and XTO Energy also performed and reported a failed test on one unfractured vertical well in the middle Bakken. The failed tests in Bakken might be owing to the heterogeneous matrix and complex geology. In addition, BHP Billiton, Marathon Oil, and Core Laboratories are also conducting field pilots in different unconventional reservoirs, but no public data are available yet.

Some researchers analyzed field pilots based on some limited publicly-available data. Hoffman and Evans [4] evaluated the unconventional Bakken IOR projects conducted in Montana and North Dakota by analyzing the data collected from seven pilot projects, including three water injection pilots, two CO_2 huff-n-puff pilots, CO_2 flooding, and natural gas flooding. It was found that injectivity was not an issue for all the pilots; however, it was unclear whether the favorable infectivity was due to the increased conductivity caused by hydraulic fractures. Early breakthrough was a common issue, probably because the massive hydraulic fractures have caused the wells to link up. Overall, most pilots did not have any increase in oil production and, based on the results, recommendations for future IOR pilot projects were proposed by the authors, including drilling additional new wells per pilot for injection, testing injectivity in these unstimulated wells, conducting core flooding experiments, and performing simulations in advance to address issues that may arise during the pilot. Later on,

Hoffman [64] evaluated seven single-well and multi-well pilot projects in the Eagle Ford based on the published data by the Texas Railroad Commission (TRC). For these cases, lean natural gas or richer hydrocarbon gases were injected in different pilots through a huff-n-puff gas injection scheme. Most pilots resulted in a 17–30% increase in cumulative production, and 30–70% improved oil production owing to gas injection was predicted in 10 years.

3. Shale Gas Reservoir

In recent years, natural gas market share of consumption has been continuously increasing owing to the advanced horizontal well technique combined with the intensive hydraulic fracturing, which made the natural gas in thin and tight shale deposits attainable. The Shale gas reservoir is analogous to coalbed methane in terms of the gas occurring status in low-permeability organic-rich formation. The primary differences between these two unconventional gas reservoirs are in their physio-chemical properties, reflected in the amount and type of organic matter, reservoir permeability, the proportion of adsorbed gas and free gas, and the thickness of gas-bearing formation [65,66], as tabulated in Table 3. A report released in 2013 indicated that the assessment of technically-recoverable shale gas reached 7299 trillion cubic feet, taking up 32% of the total natural gas resources [24]. With an estimated 665 trillion cubic feet, the United States ranked fourth to China, Argentina, and Algeria, for which the estimated natural gas resources were at 1115, 802, and 707 trillion cubic feet, respectively. In the United States, shale gas plays with remarkable reserves take up considerable portions of unconventional gas resources. Barnett shale, located in the Fort Worth Basin of North Texas, is the most developed shale gas play in the U.S. [67]. As the largest onshore natural gas formation in Texas, Barnett shale contains 43 trillion cubic feet of technically-recoverable natural gas [68]. Haynesville Shale formation is located in Northwest Louisiana, Southwestern Arkansas, and Eastern Texas and covers an area of approximately 9000 square miles. In April 2017, the energy resource assessment in Haynesville formation was revised by United States Geological Survey (USGS) and the updated accumulations included 304.4 trillion cubic feet of natural gas, 4.0 billion barrels of oil, and 1.9 billion barrels of natural gas liquids [69]. Fayetteville Shale within the Arkoma Basin of Arkansas and Oklahoma encompasses over 5000 square miles, ranging in depth between 1500 to 6500 feet with a thickness from 50 to 550 feet [70]. The agency estimated that 32 trillion cubic feet of technically-recoverable natural gas was remaining in the shale play [68]. Driven by the boom of shale gas resources development and the low price for natural gas, the U.S. natural gas-fired electricity generation surpassed coal-fired generation for the first time in 2015 [71].

Table 3. Physio-chemical differences of the coalbed methane reservoir and the shale gas reservoir.

Properties	Coalbed Methane Reservoir	Shale Gas Reservoir
Organic matter (wt%)	>50	<50
Type of organic matter	Vitrinite/inertinite macerals	Liptinite
Methane existing status	Sorbed gas (98%)	Sorbed gas, free gas
Sorbed gas content (m^3/ton)	1–25	<10
Matrix permeability (md)	1–50	10^{-5}–1
Thickness (ft)	4–110	30–300
Young's modulus (psi)	$(0.1–1) \times 10^6$	$(3–8) \times 10^6$

3.1. Enhanced Gas Recovery (EGR) Methods

Natural gas exists in the tight and organic-rich shale reservoirs in three states: free gas in natural fractures, adsorbed gas in matrix, and dissolved gas in kerogen and bitumen. Currently, the accessible technique to unlock the gas resources from shale formation is primary depletion, which is possible through horizontal drilling combined with intensive fracturing. However, a sharp decline after a few years of production, as shown in Figure 5 [72], indicates the necessity for applying enhanced gas recovery (EGR) methods. Carbon dioxide has an adsorption preference over methane in shale reservoirs

and it can be trapped in organic compounds by being sorbed at the rock surface [73]. CO_2 injection into shale reservoirs is not only proposed as a technique to improve natural gas recovery through CO_2 adsorption and CH_4 desorption, but also is considered as a potential resource for underground anthropogenic carbon dioxide storage and sequestration. In this section, we review the laboratory measurements of physio-chemical properties of shale rock with methane and other injectants, field-scale simulations of CO_2–EGR in shale gas reservoir, and in-situ CO_2 injection pilots for EGR.
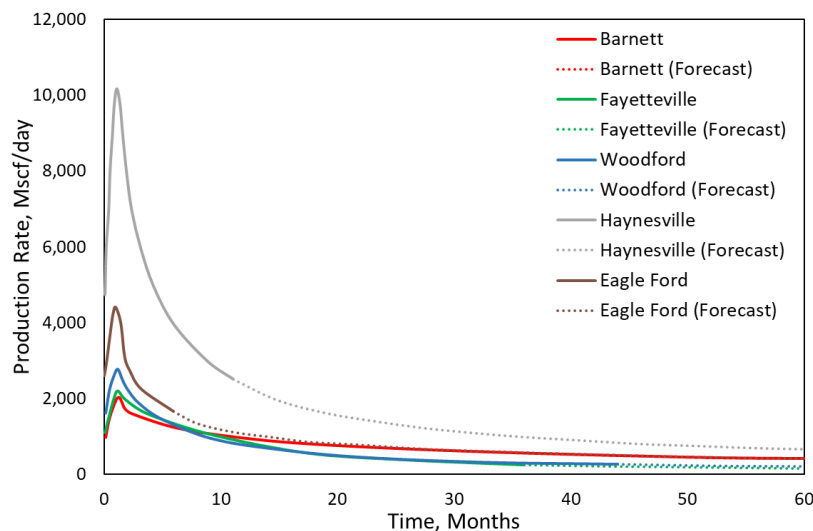

Figure 5. Absolute averaged daily gas production rate per well for different shale gas formations. Reprint with permission [72], 2015, Society of Petroleum Engineers.

3.1.1. Physio-Chemical Properties Measurements

Gas adsorption- or desorption-induced swelling or shrinkage of shale can affect the pore structure and have an impact on gas transport in shale [74,75]. Recently, many studies focused on the change of physio-chemical properties of shale due to carbon dioxide (or other gases) injection. The adsorption capacities of different gases [74–78], adsorption-induced swelling strain and swelling rate [77,79,80], gas diffusion in shale [76,81], and physical and chemical structure change [82] have been investigated in different studies.

The measured adsorption capacities of N_2, CH_4, and CO_2 in shale were in an ascending order (e.g., 1:3.2:9.3 at 7MPa and 328.2 K), but one order of magnitude smaller compared to adsorption capacities in coal [74,78]. The lower adsorption capacity in shale was owing to the lower total organic carbon content (55%) and the high level of ash content (90%) [78]. Most studies indicated that the absolute adsorption amount of CO_2 in shale is two to five times larger than that of CH_4 [74,77,78,83]. In addition, dry sample could result in a much larger absolute adsorption capacity compared to a moist sample, indicating that a water environment could strongly reduce CO_2 storage capacity in a shale reservoir [76].

The gas adsorption capacities in shale could also affect the adsorption-induced swelling strain. The measurement of adsorption-induced swelling strain in shale was deemed to be more difficult than in coal because: 1) The shale strain was positively correlated to gas uptake [76], as gas adsorption capacity in shale was one order of magnitude less than in coal; therefore, gas adsorption-induced volumetric swelling strain in matrix was expected to be not as large as in coal; and 2) shale was stiffer compared to coal [77]. Chen et al. [79] studied the strain behavior of shale in methane and reported that the measured volumetric swelling strain of shale at pressure of 10 MPa was one order of magnitude smaller than that of coal. Lu et al. [71] measured the volumetric strain of shale rock in CO_2 and divided the strain behavior at a given pressure into three regions: transient shrinkage, slow swelling, and stable strain. It was found that the strain increased with pressure before the pressure reached the CO_2 critical pressure. After that, increasing pressure resulted in a decrease in strain, primarily because CO_2

swelling was decreased with increasing pressure at supercritical state. Chen et al. [74] indicated that the measured swelling rate of shale in non-adsorbing gas (helium) was higher than that in adsorbing gases (N_2, CH_4, and CO_2). The swelling rate of shale in CO_2 had the lowest value owing to the slow CO_2 diffusion in shale and the property change of CO_2 during phase transition from vapor to liquid.

Viscous flow, molecular diffusion, Knudsen diffusion, and surface diffusion described the gas transport behaviors in porous media and were generally evaluated based on different pore sizes, pressure, and production stages [74,76,81,84,85]. A schematic diagram of different flow types and particle motion within a given flow regime is shown in Figure 6 [84]. Fathi and Akkutlu [13,18] concluded that free gas transport in macropores was driven by viscous flow, molecular diffusion (molecule–molecule collision), and Knudsen flow. Wu et al. [85] also concluded that gas transport was primarily dominated by viscous flow in meso-macropores at high pressure (contribution up to 99%); but the contribution of viscous flow in micropores can be ignored. Moreover, Knudsen diffusion (molecule–wall collision) made great contribution to gas transfer in meso-macropores at low pressure. Yuan et al. [76] calculated diffusivities in macropores and micropores, which were in the order of 10^{-9} and 10^{-14} m^2/s, respectively. The diffusion mechanisms were assumed to be molecular diffusion in macrospores, which made contributions in the early production stage, and Knudsen diffusion in micropores, which played an important role in a later recovery stage. This finding (Knudsen diffusion being dominant in micropores) was inconsistent with the conclusion in other studies, indicating that Knudsen diffusion played an important role in meso-macropores only [13,18,85]. Many researchers concluded that surface diffusion (particle–solid surface collision) made the most contributions (>90%) in adsorbed-gas transport in micropores [13,81,85–87]. Unlike the slippage effect or Knudsen effect, which are driven by small pore size, surface diffusion was driven by density gradient of the adsorbed-gas [87]. A positive correlation was found between surface diffusion and reservoir pressure or temperature [81,85]. In addition, the presence of water could reduce gas diffusivities in both macro- and micropores and affect gas flow behavior in a shale reservoir [76].
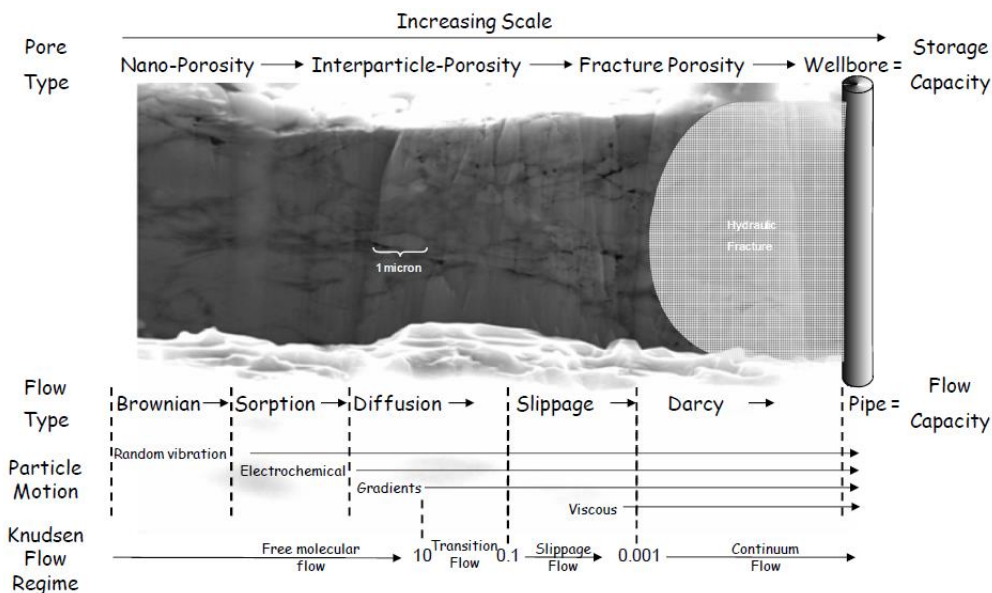

Figure 6. Flow types, particle motion within a given flow regime. The cross sectional image is a SEM image of a shale gas sample. Reprint with permission [84], 2010, Society of Petroleum Engineers.

3.1.2. Field-Scale Simulation Study

Many researchers used different simulation models to examine the feasibility of CO_2–EGR methods (gas flooding or huff-n-puff gas injection) in shale gas reservoirs.

Some simulation results indicated that gas flooding [19,20,88–90] and huff-n-puff [13] approaches for EGR were promising for enhanced gas recovery.

Kalantari-Dahaghi [20] used a dual-porosity compositional simulation model to simulate CO_2 flooding in a shale gas reservoir, where the reservoir permeability was 40 nanodarcy, while the instant sorption model and a time dependent sorption model were examined and compared. After five years of primary production, the two producers were shut-in and CO_2 was injected into another horizontal well for five years. Simulation results indicated that no CO_2 was produced from the two producers in 20 years of gas production. The author explained that the preferential adsorption of CO_2 allowed methane to be released from the formation, resulting in a feasible methane recovery, and a successful CO_2 sequestration in the matrix. In our view, the increase in methane production could be the result of the gas injection-induced reservoir re-pressurization, rather than due to the CO_2 adsorption effect. Moreover, no CO_2 appearing at the production well may be owing to the shale matrix being too tight (40 nanodarcy) and CO_2 not being able to migrate to the producer. Here, it is suggested to perform another two simulation cases: (i) injecting N_2 (with lower adsorption capacity than CH_4 in shale) and (ii) primary depletion without gas injection, and compare the results with CO_2 flooding to examine the mechanisms of CO_2/CH_4 adsorption/desorption and reservoir re-pressurization for EGR, respectively.

Godec et al. [88] used the COMET3 simulator to model CO_2 flooding in a shale play based on the Marcellus shale history-matched data. The adsorbed contents of methane and CO_2 were calculated by using the available Langmuir equilibrium isotherm data from Marcellus at the depth of 1728 m. Simulation results indicated that the cumulative gas production was increased 7% due to CO_2 injection. Sun et al. [19] proposed a dual-porosity mathematical model and adopted a five-spot well pattern to simulate CO_2 flooding in a shale gas reservoir. The mechanisms of viscos flow, Knudsen diffusion, and molecular diffusion were incorporated in the model, and gas adsorption and desorption in the matrix were considered using the extended Langmuir isotherm equation. The results indicated higher injection pressure led to a higher recovery factor, but also accelerated CO_2 transport and shortened the CO_2 breakthrough time. Three stages were characterized in CO_2 sequestration and enhanced gas recovery process: early depressurization production period, intermediate period of CH_4 desorption with CO_2 adsorption, and late period of CH_4 and CO_2 production simultaneously. Yu et al. [89] used a GEM simulator and incorporated the extended Langmuir isotherm to examine both CO_2 flooding and huff-n-puff injection in the Barnett shale reservoir (with permeability of 500 nd). They observed that the CO_2 flooding increased the CH_4 recovery by more than 2% and the conclusion was that re-pressurization was the primary mechanism for the CO_2–EGR process. Kim et al. [90] performed CO_2 flooding in a shale reservoir based on the history-matched data from Barnett shale, with the mechanisms of multi-component adsorption, molecular diffusion, and dissolution incorporated in the simulation model. The results indicated that after 40 years of production, only 4% of injected CO_2 was produced, leaving a huge amount of CO_2 stored in the reservoir.

Fathi and Akkutlu [13] proposed a triple-porosity single-permeability simulation model to study multi-component transport in a shale reservoir with the permeability of 100 nd. A shale gas flow model was built to investigate CO_2 huff-n-puff injection in a single horizontal well with multiple fractures. The simulation included 10 years of primary production, five years of CO_2 injection, a short soaking time, and 30 years of final production. In the huff-n-puff production period, the total methane recovery reached up to 85% and only less than 10% of the CO_2 was produced. The results indicated that counter-diffusion (molecules diffuse in opposite directions) and competitive adsorption of CO_2 over CH_4 were the important mechanism in the organic microspores for EGR.

In some simulation studies, CO_2 huff-n-puff [89,91] for EGR were not effective in shale gas reservoirs. Yu et al. [89] found the recovery for huff-n-puff CO_2 injection was lower than the one without CO_2 injection. They explained that the unfavorable performance for CO_2 huff-n-puff was because of a large amount of CO_2 (96%) flowing back to the surface in the puff stage without carrying out much CH_4 and the CO_2 adsorption effect was negligible. Eshkalak et al. [91] numerically compared the efficiency of hydraulic re-fracturing treatment to CO_2–EGR approaches (flooding and huff-n-puff) to improve gas production in shale with reservoir permeability of 100 nd. The simulation results indicated that for the CO_2 huff-n-puff injection, after the five-year shut-in period, almost all the injected CO_2

(96%) was produced back. In addition, the hydraulic re-fracturing treatment well outperformed the CO_2 flooding scheme due to the high fracture conductivity and effective drainage area. However, CO_2 flooding might have a pronounced effect in long-term enhanced gas recovery, it was recommended that re-fracturing should be applied at first, followed by CO_2 flooding at a later time. It should be noted that in this study they found that using the adsorption isotherms (BET multi-layer or Langmuir isotherms) had a negligible effect on EGR, and this observation can explain the large amount of CO_2 flowing back with produced nature gas in the puff process. It should be noted that, diffusion mechanisms were not included in either of the models [89,91]. This probably is one reason to explain the unfavorable huff-n-puff approach for EGR as well as the large amount of CO_2 flow back. The simulation studies about different gas injection approaches in shale gas reservoirs for EGR are tabulated in Table 4.

3.2. Gas Injection-Enhanced Recovery Mechanisms

Gas migration behavior in organic pores or fractures is crucial to understand the mechanisms of CO_2–EGR and CO_2 sequestration in organic-rich shale gas reservoirs. The mechanisms of gas storage and transport in a shale gas reservoir is highly dependent on organic content, pore structure, and temperature [87]. For the absorbed gas stored in organic-rich micropores, surface diffusion plays the dominant role in releasing the adsorbed molecules from the micropore walls. For the free gas occurring in macropores or fractures, at a lower pressure and a higher temperature, as the molecular mean path is larger than the effective pore throat diameter, gas transfer is governed by the gas slippage effect or Knudsen diffusion. When intermolecular collision becomes strong enough (with a small Knudsen number), the conventional viscous (Darcy) flow is the gas transport mechanism. Carbon dioxide has a stronger adsorption affinity (two to five times) over methane in organic-rich shale. The clay minerals, such as illite, with micropore structures provide a suitable gas storage environment for CO_2 storage [66]. The injected CO_2 contributes to releasing and displacing methane from the micropore walls of organic shales, making the EGR possible. However, the salinity of connate water could reduce the EGR performance by decreasing the dispersion coefficient of CO_2 into CH_4 [92]. In addition, the intrinsic heterogeneity of shale rock generally negatively affects gas production in primary depletion [93,94]; however, it is expected to play a positive role in huff-n-puff gas injection EGR, similar to oil shale EOR [5,7,16,37,94]. A similar performance has also been reported for conventional rocks [95], as injection of the CO_2 and CH_4 mixture in heterogeneous carbonate rocks outperformed the same EOR process in homogeneous sandstones.

The effect of matrix permeability on EGR as well as on CO_2 sequestration is examined by plotting the increased gas recovery factor versus matrix permeability in Figure 7a,b. Different colors represent different simulation works in Table 4. An improved gas recovery is seen for both huff-n-puff and gas flooding in such ultra-tight nanoscale permeability shales. The application of a dual/triple porosity dual permeability system is perceived as a significant contribution to the favorable EGR process. Well-developed natural fractures and intensive hydraulic fractures enhance the reservoir permeability to some degree, allowing gas to penetrate further, which is especially important for the gas flooding scheme. Moreover, diffusion may play an important role in the huff-n-puff process. In some studies, disregarding diffusion resulted in a reduced gas recovery factor [89]. CO_2 could be successfully captured in shale gas reservoirs through both gas injection regimes. For gas flooding, the distance between injection and production wells could strongly affect the methane recovery as well as CO_2 storage [88].

Table 4. The simulation studies about different gas injection approaches in shale gas reservoirs for EGR.

|												
						Simulation Study						
Injection Gas	Formation	K (nd)	ϕ	Natural Fracture	Hydraulic Fracture	Method	Model	Adsorption Isotherm	Diffusion	Increased Gas RF (%)	Sequestrated CO_2 (%)	Reference
CO_2		40	0.05	0.4 μD	conductivity 60 mD-ft	huff-n-puff	Dual porosity dual permeability	Extended Langmuir	Yes	≈147	100	[20]
CO_2	Marcellus Shale	100–1000 (average 520)	0.05–0.1 (average 0.7)	2.5 μD	-	flooding	Triple porosity dual permeability	Langmuir	Yes	11.4–0 (well distance ranges 15 m–229 m)	34.5–100 (well distance ranges 15 m–229 m)	[88]
CO_2	-	100	0.05	spacing 0.05 m width 5 μm	NA	flooding	Dual porosity	Langmuir	Yes	35.2 (P_{inj} = 6MPa) 51.4 (P_{inj} = 7MPa)	51.57 60.3	[19]
CO_2	-	100	0.00532 (organic) 0.00798 (in-organic) 0.0133 (fracture)	NA	-	huff-n-puff	Triple porosity single permeability	Extended Langmuir	Yes	35	90	[13]
CO_2	Barnett Shale	0.58	0.029	7.12 μD	-	flooding	Dual porosity dual permeability	Extended Langmuir	Yes	12	50	[90]
CO_2	Barnett Shale	500	0.06	-	constant finite conductivity	flooding huff-n-puff	Dual permeability	Extended Langmuir	No	2.95, 2.87 −4.7, −4.1	99 4	[89]
CO_2	-	100	0.05	-	conductivity 10 mD-ft	huff-n-puff flooding flooding re-fracturing	Dual porosity dual permeability	BET/Langmuir No BET/Langmuir -	No	<4 ≈9 ≈31 ≈185	4 -	[91]
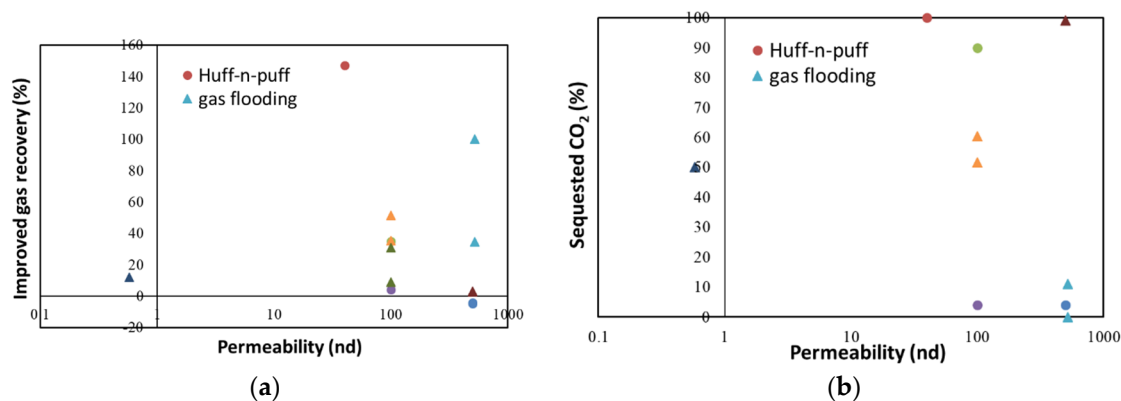
Figure 7. (**a**) Incremental gas recovery factor and (**b**) sequestrated CO_2 through huff-n-puff and gas flooding from simulation studies (Table 4), for the range of matrix permeability from 0.1 to 1000 nd. Different colors represent different simulation works.

3.3. CO_2 Injection Field Pilots

Preliminary investigation about CO_2 injectivity and storage potential in shale gas formation has been conducted in different studies [88,96,97]. The concept of enhancing gas recovery from CO_2 injection in shale formation was encouraging, but only a few field pilots about CO_2 injection in shale formation have been reported [98,99].

Nuttall et al. [98] performed a small-scale field pilot for CO_2 injection at Devonian Ohio Shale, eastern Kentucky. CO_2 storage capacity in this shale formation was estimated up to 28 Gt and up to 100 tons of CO_2 was injected into a vertical well in three days; however, the injection was terminated because of a packer failure. Louk et al. [99] performed an in-situ test in the Chattanooga Shale formation in Morgan County, Tennessee, which was the first successful field trial of CO_2 huff-n-puff gas injection. In this project, approximately 510 tons of CO_2 was injected into six candidate horizontal wells at the depth from 2550 to 3675 feet. After soaking for four months, gas flow rate was increased over eight times in the first month. More valuable natural gas liquid (NGL) was produced with CO_2 and methane, indicating that injection of CO_2 could effectively alleviate condensate blockage in gas-condensate shale reservoirs. They reported that a total of 41% of injected CO_2 was produced during the 17 months of flowback phase and more than half of the CO_2 was stored in the formation.

4. Shale Condensate Reservoirs

4.1. Distribution and Reserves

Gas condensate, also called condensate, or natural gas condensate, is a light and gassy low-density liquid and generally occurs in association with gaseous hydrocarbons. In gas-condensate reservoirs, the fluid is initially in the gas phase as the initial reservoir pressure is above the dew-point pressure. In the production process, gas condenses into liquid phase as pressure decreases below the dew-point pressure. Owing to the development of the horizontal well and multi-stage hydraulic fractures, an enormous amount of shale gas condensate has been produced from Texas in Eagle Ford and Permian formations, to Pennsylvania in Marcellus and Utica plays. In the U.S., gas condensate is commonly treated as crude oil, especially when it comes to the reserves and output. The Eagle Ford condensate zone was estimated to be 890 square miles with an average estimated ultimate recovery (EUR) of 4.5 billion cubic feet [68]. In recent years, a continuous increase in condensate production has been seen from Eagle Ford formation. From 2009 to 2012, the U.S. condensate production rose by 54%, from 178 million barrels to 274 million barrels, among which the Eagle Ford play contributed to almost 90% of the production [100].

4.2. Enhanced Recovery Methods

In shale gas-condensate reservoirs, when reservoir pressure drops below the dew-point pressure, the condensate accumulates near the wellbore, leading to a reduction in both gas relative permeability and gas production. This phenomenon, which is called retrograde condensation [101], heavily impedes the fluid flow from reservoir to the wellbore. One commonly used method to restore gas productivity after condensate blocking is to inject dry gas [102]. The purpose is to increase or maintain reservoir pressure above the dew-point pressure to re-vaporize the condensate and prevent condensate formation. The injected gas could be methane, CO_2, N_2, or produced gas (flaring/venting gas). A series of studies on gas injection, including gas flooding and huff-n-puff injection in shale condensate reservoirs were conducted either numerically or experimentally [6,103–107]. Overall, there are a few attempts to study gas injection in shale gas condensate reservoirs, primarily because overcoming the condensate-blocking issue is more challenging in low-permeability unconventional formations.

4.2.1. Gas Flooding

There are a few articles which discuss simulation and experimental studies of gas flooding in shale condensate reservoirs and compare them to huff-n-puff gas injection. Sheng [107] numerically examined and compared three scenarios of methane flooding, huff-n-puff methane injection, and primary depletion in Eagle Ford shale condensate reservoirs with hydraulic fractures. The results showed that huff-n-puff injection was more effective in condensate production than gas flooding and primary depletion. Meng et al. [6] experimentally compared the efficiency of methane flooding to huff-n-puff methane injection using synthetic gas-condensate (85% methane and 15% n-butane)-saturated Eagle Ford cores. Huff-n-puff injection without a shut-in period achieved a higher recovery factor (25%) than gas flooding (19%).

The inefficient gas flooding in shale condensate is primarily owing to the characteristics of shale reservoir (low porosity and ultra-low permeability), and the properties of condensate fluids. In order to re-vaporize the condensate near the wellbore, and at the same time alleviate condensate blockage, a faster pressure is required to be built up near the production well. However, because of the low-injectivity in shale, it takes a much longer time for the injection gas to migrate from the injector to the production well.

4.2.2. Huff-N-Puff Gas Injection

Investigation of huff-n-puff gas injection and optimization of parameters in huff-n-puff for enhanced shale condensate recovery have been conducted in some simulation and experimental studies. Most studies concluded that a soaking period was not necessary in the huff-n-puff process and might have a negative effect on condensate recovery [6,104,107]. Especially when the injection pressure was not much higher than the dew point pressure, a shut-in period may lead to a reformation of condensate in the near-well formation [104]. This is because the pressure drop during the soaking period leads to a reformation of condensate in the near-well formation.

For a constant production time, longer injection time resulted in longer pressure build-up time, which allowed more condensate to be re-vaporized and a higher recovery factor was achieved; however, it also demanded for a large amount of injectants and increased the cost and reduced the profit [104]. One simulation study [105] indicated that the best performance was achieved when the huff time and puff time were set identical. From a practical point of view, in terms of quicker return on investment, a relatively shorter huff time was suggested. Another similar simulation study [106] also indicated that a shorter injection period led to a higher recovery factor. Some studies indicate that more cycle numbers are favorable for cumulative condensate recovery. In spite of the fact that the incremental recovery was reduced with cycle numbers, it was still higher than the primary depletion recovery [104]. However, it is necessary to optimize the cycle number from a profitability standpoint.

One simulation work [105] examined three injectants (CH_4, CO_2, and N_2) for huff-n-puff on enhanced condensate recovery performance and indicated that CO_2 and CH_4 injections resulted in almost the same oil recovery factor (42%), and both CO_2 and CH_4 outperformed N_2 injection (recovery factor of 29%) as it was difficult to mix N_2 with the condensate. In another research study, Sharma and Sheng [108] performed a core-scale simulation based on a lab study to examine a huff-n-puff gas injection on shale condensate recovery by using four injectants (methane, ethane, methanol, and isopropanol), and it was reported that ethane resulted in higher and faster recovery. Both methane and ethane could effectively re-vaporize the condensate, but ethane also reduced dew point pressure and resulted in the same recovery factor as methane, with a relatively small injectant volume and time.

While most simulation studies on huff-n-puff gas injection in condensate shale reservoirs did not consider molecular diffusion and nanoconfinement effects in their models [104,105,108], Jiang and Younis [107] combined these two effects as well as gas sorption in their compositional simulation model. The results indicated that inclusion of the capillary pressure effect increased the overall dew point pressure, which was consistent with a previous study [109], resulting in a more severe condensate blockage. They also reported that molecular diffusion made little contribution to condensate production, while desorption increased the condensate recovery.

The experimental and simulation studies about huff-n-puff and gas flooding approaches in shale condensate reservoirs for enhanced condensate recovery are tabulated in Table 5. Among the mechanisms of huff-n-puff gas injection in shale condensate, re-vaporization of the liquid into a gaseous phase in the huff period was taken as one of the most important ones, which can also alleviate condensate blockage near the wellbore. Huff-n-puff injection creates a quick pressure response to the gas injection near the wellbore. Re-pressurization of reservoir formation and a large pressure difference, or a high drawdown pressure between the reservoir and well flowing pressure, is another mechanism for enhanced condensate recovery.

Table 5. The experimental and simulation studies about different gas injection approaches in shale condensate reservoirs for enhanced condensate recovery.

Experimental Study										
Condensate Sample	Injection	Rock Sample	K (μd)	Porosity (%)	Method	P_{inj} (psi)	T (°F)	Production Time	Condensate RF (%)	Reference
synthetic gas-condensate mixture: 85% C_1 +15% n-C_4	C_1	Eagle Ford outcrop	0.1	6.8	huff-n-puff gasflooding	1900	68	30 min	25 19	[6]
synthetic gas-condensate mixture: 85% C_1 +15% n-C_4	C_1	Eagle Ford outcrop	0.1	6.8	huff-n-puff	2200	68	-	10.7 1st, 8.7 2nd, 5.53 3rd, 5.4 4th, 5.185 5th	[103]
Simulation Study										
Condensate Sample	Injection	Formation	K (uD)	Porosity (%)	Method	P_{inj} (psi)	T (°F)	Production Time	Increased Condensate RF (%)	Reference
Eagle Ford Condensate	C_1	Eagle Ford	0.1	6	huff-n-puff	4000	200	200 d	≈0.3% (10d inj), 1.5% (50d inj), 2.1% (100d inj)	[104]
Eagle Ford Condensate	C_1 85% C_1 + 15% C_2 CO_2	Eagle Ford	0.1	6	gas flooding huff-n-puff gas flooding huff-n-puff gas flooding huff-n-puff	9500	310	100 d	5.23 13.93 4.377 16.18 −1.467 11.092	[107]
Eagle Ford Condensate	C_1 CO_2 N_2	Eagle Ford	0.3	5.6	huff-n-puff huff-n-puff huff-n-puff	9985	270	300 d	13.935 14.068 0.875	[105]

5. Greenhouse Gas Control

Carbon dioxide is a powerful greenhouse gas and has long residence time in the atmosphere. Anthropogenic carbon dioxide emissions have been greatly accelerated as our energy needs strongly depend on fossil fuels. It was reported that the average growth rate of CO_2 emissions increased from 1.1% per year for 1990–1999 up to 3% per year for 2000–2004 [110]. Some options have been suggested for geological storage of carbon dioxide, such as deep saline aquifers, depleted oil and gas fields, unmineable coalbeds, and deep oceans [111]. Methane, as another greenhouse gas, is associated with a greater global warming potential compared to carbon dioxide in a short time scale [112]. In petroleum and natural gas industry, natural gas emission from the gas-bearing strata to surface occurs over a lifetime of a well during both well completion and production stage. In most of oil fields, natural gas is concurrently produced with oil during primary production; under reservoir conditions it is dissolved in the oil but as the oil is extracted and pressure drops, it is released from solution. The produced natural gas can be either recovered, reinjected to the reservoir, flared, or vented. Considering the low price of natural gas, it is not economically efficient to sell the produced gas especially where there is limited infrastructure for gas transportation available. Therefore, reservoir engineers typically flare or vent the excess produced gas—polluting the environment in the process. Flaring and venting are common practices in many oil production operations. Figure 8a shows that the amount of gas flared/vented in the U.S. has substantially increased with the development of shale resources since 2001. Based on U.S. Energy Information Administration, more than 270 billion cubic feet of natural gas was flared or vented in 2015 [113]. North Dakota, where Bakken oil shale is located, contributed to more than one third of this total.

Before 2005, there were less than 100 active producing wells in Bakken; however, this number has increased to more than 2500 wells by 2016 [114]. As Figure 8 shows, Bakken oil (and the associated gas) production increased significantly since 2005, as did natural gas flaring and venting [115]. The Energy Information Administration (EIA) reports indicated that approximately 12.85% of the produced gas from Bakken shale (equivalent to 88 billion cubic feet) was flared or vented in 2017 and no gas has been reinjected since the start of Bakken development. Flaring not only unproductively wastes energy but also emits carbon dioxide and other hazardous gases, such as CO, SO_2, NO_X, owing to incomplete combustion, as well as volatile organic compounds, impacting regional air quality [22].
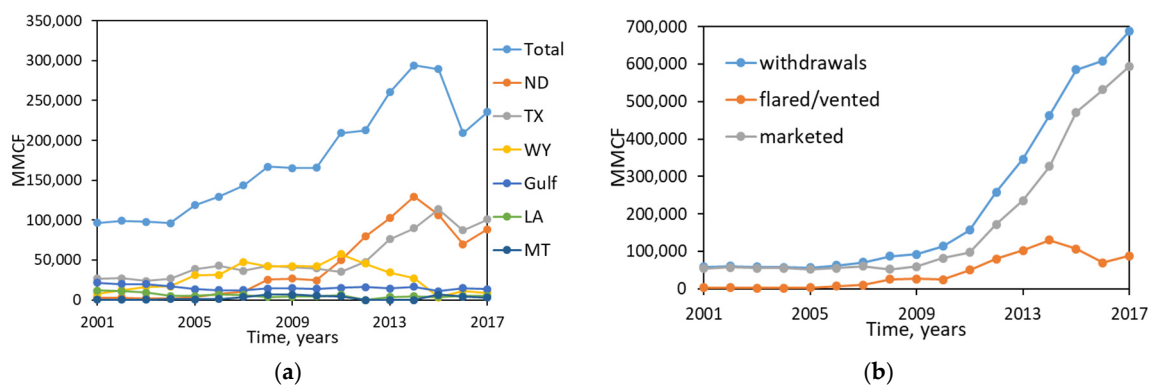

Figure 8. (**a**) Total flared/vented natural gas in United States; (**b**) P\produced, marketed, and flared/ vented natural gas in the state of North Dakota. Reproduced from [115], 2019, Energy Information Administration (EIA).

The growing increase of greenhouse gases in the atmosphere could change the climate and induce possible biological consequences [116]. It is necessary to take steps to control greenhouse gas emissions in oil industries, including reducing natural gas flaring or venting, capturing the flue gases from potential sources such as power plants, cement plants, and oil refineries, and reinjecting the produced gases and flue gases into reservoirs for enhancing oil or gas recovery (EOR/EGR) and simultaneously storing greenhouse gases in the reservoir formation permanently. Clearly flaring needs

to stop and reinjection of produced gas back in the shale formation is a viable solution. However, initiating a gas-reinjection and/or CO_2 storage global revolution will face financial constraints and challenges especially for smaller operators. Flaring reduction and underground CO_2 storage will be effectively possible only if it is cost effective and can create markets. To create wide-scale uptake of gas storage research studies in shale reservoirs, one needs to provide convincing evidence that reinjecting the produced gas and/or CO_2 injection not only reduces emissions, but also will help improve oil production, thereby underpinning the economic argument.

In consideration of the subsurface geological sequestration of anthropogenic carbon dioxide, some necessary characteristics for gas storage should be examined, such as gas storage capacity, trapping mechanism, gas migration and possible leakage, and infrastructure for gas transport from the surface to underground [87]. Although shale reservoirs are currently in primary depletion, many favorable experimental and simulation results and a number of successful gas injection EOR pilots indicated there is potential for gas injections in shale reservoirs for EOR and EGR. Gas injection not only could enhance oil or gas recovery under the mechanisms of re-pressurization, diffusion, re-vaporization, and desorption, but the significant amount of carbon dioxide could also be trapped in kerogen-rich shale reservoirs, which have a large storage capacity with tremendous nanopores acting as molecular sieves to safely and permanently store CO_2 in an adsorbed state [117].

Aside from above-mentioned targets for CO_2 sequestration in unconventional reservoirs, a CO_2 fracturing technique that participates in commercial-scale tight shale oil and gas production could also contribute to CO_2 storage to some degree [118,119]. In comparison with water-based fracturing, CO_2 fracturing significantly reduces or completely eliminates the water usage [120], resulting in a low-water saturation environment near the wellbore, which is favorable for oil or gas mobility in tight shale formation.

6. Conclusions and Final Remarks

In this paper, we have reviewed the current research progress regarding gas injection in shale reservoirs for enhanced oil/gas recovery (EOR/EGR) and subsurface geological sequestration of greenhouses gases. Huff-n-puff and gas flooding are suggested as potential approaches for EOR/EGR in shale reservoirs based on experimental studies and simulation results. The effectiveness of huff-n-puff injection is more pronounced in comparison with gas flooding owing to its quick response to gas injection and larger pressure difference between reservoir pressure and wellbore pressure. Injection of carbon dioxide and produced gas (flaring or venting gas in oilfields) shows favorable oil recovery. In spite of the fact that field data are limited, many oil companies are directing efforts towards conducting field pilots to verify the feasibility and profitability of gas injection in oil-rich shale reservoirs. Finally, gas utilization through reinjection, as a substitute for flaring or venting in shale reservoirs for EOR has been addressed.

Although multiple research efforts have been made to examine the effectiveness of gas injection to enhance recovery of shales, our knowledge regarding gas injection EOR/EGR methods for such resources is still limited. CO_2 sequestration and greenhouse gas reduction approaches are not practically being performed at the field-scale and there is still a gap between oil and gas industries and the environmental stakeholders. Filling this gap is inevitably important as our energy needs still depend on fossil fuels and, at the same time, we are responsible for protecting the local, regional, and global environment. Further research is essential to provide environmentally friendly enhanced recovery methods for shale oil and gas resources, and to help the environmental agencies and petroleum business to find mutual interests.

Conflicts of Interest: The authors declare no conflict of interest.

Nomenclature

D_{ij}	binary diffusion coefficient between component i and j [cm^2/s]
D_{ik}	diffusion coefficient of component i in phase k [cm^2/s]
D_{eff}	effective diffusion coefficient in a porous media [cm^2/s]
$\overline{\overline{K}}_{ik}$	dispersivity coefficient of component i in the phase k [cm^2/s]
M_i	molecular weight of component i [g/mol]
$M_{ik}{}'$	the molecular weight of solvent [g/mol]
P_{ci}	critical pressure of component i [atm]
R	universal gas constant [cm^3·atm/(K·mol)]
S_k	saturation of phase k
T	temperature [K]
T_{ci}	critical temperature of component i [K]
u_k	Darcy's flow velocity [cm/s]
v_{ci}	critical volume of component i [cm^3/mol]
v_{bi}	partial molar volume of component i at the boiling point [cm^3/mol]
y_{ik}	mole fraction of component i in phase k
$\overline{\alpha}_k$	dispersivity of phase k in the three directions [cm]
ϕ	porosity
μ_k	viscosity of phase k [cp]
ρ_k	molar density of phase k (k = oil, gas) [mol/cm^3]
ρ_{kr}	reduced density of phase k
σ_{ij}	collision diameter
τ	tortuosity factor
ω	acentric factor
Ω_{ij}	collision integral of the Lennard-Jones potential

References

1. Energy Information Administration (EIA). Even as Renewables Increase, Fossil Fuels Continue to Dominate U.S. Energy Mix. 2017. Available online: https://www.eia.gov/todayinenergy/detail.php?id=31892 (accessed on 31 October 2018).
2. Energy Information Administration (EIA). Technically Recoverable Shale Oil and Shale Gas Resources: An Assessment of 137 Shale Formations in 41 Countries outside the United States. 2013. Available online: https://www.eia.gov/analysis/studies/worldshalegas/pdf/overview.pdf (accessed on 31 October 2018).
3. Energy Information Administration (EIA). Future U.S. Tight Oil and Shale Gas Production Depends on Resources, Technology, Markets. 2016. Available online: https://www.eia.gov/todayinenergy/detail.php?id=27612 (accessed on 31 October 2018).
4. Hoffman, B.T.; Evans, J.G. Improved oil recovery IOR pilot projects in the Bakken formation. In Proceedings of the SPE Low Perm Symposium, Denver, CO, USA, 5–6 May 2016.
5. Chen, C.; Balhoff, M.; Mohanty, K.K. Effect of reservoir heterogeneity on primary recovery and CO$_2$ huff 'n' puff recovery in shale-oil reservoirs. *SPEREE* **2014**, *17*, 404–413. [CrossRef]
6. Meng, X.; Sheng, J.J.; Yu, Y. Experimental and numerical study of enhanced condensate recovery by gas injection in shale gas–condensate reservoirs. *SPEREE* **2017**, *20*, 471–477. [CrossRef]
7. Gamadi, T.D.; Elldakli, T.F.; Sheng, J.J. Compositional simulation evaluation of EOR potential in shale oil reservoirs by cyclic natural gas injection. In Proceedings of the Unconventional Resources Technology Conference, Denvor, CO, USA, 25–27 August 2014.
8. Hoffman, B.T. Comparison of various gases for enhanced recovery from shale oil reservoirs. In Proceedings of the Eighteenth SPE Improved Oil Recovery Symposium, Tulsa, OK, USA, 14–18 April 2012.
9. Yu, Y.; Li, L.; Sheng, J.J. A comparative experimental study of gas injection in shale plugs by flooding and huff-n-puff processes. *J. Nat. Gas Sci. Eng.* **2017**, *38*, 195–202. [CrossRef]

10. Jin, L.; Hawthorne, S.; Sorensen, J.; Pekot, L.; Bosshart, N.; Gorecki, C.; Steadman, E.; Harju, J. Utilization of produced gas for improved oil recovery and reduced emissions from the Bakken formation. In Proceedings of the SPE Health, Safety, Security, Environment, & Social Responsibility Conference, New Orleans, LA, USA, 18–20 April 2017.

11. Jin, L.; Hawthorne, S.; Sorensen, J.; Pekot, L.; Kurz, B.; Smith, S.; Heebink, L.; Bosshart, N.; Torres, J.; Dalkhaa, C.; et al. Extraction of oil from the Bakken shales with supercritical CO_2. In Proceedings of the SPE/AAPG/SEG Unconventional Resources Technology Conference, Austin, TX, USA, 24–26 July 2017.

12. Li, L.; Sheng, J.J. Upscale methodology for gas huff-n-puff process in shale oil reservoirs. *J. Pet. Sci. Eng.* **2017**, *153*, 36–46. [CrossRef]

13. Fathi, E.; Akkutlu, I.Y. Multi-component gas transport and adsorption effects during CO_2 injection and enhanced shale gas recovery. *Int. J. Coal. Geol.* **2014**, *123*, 52–61. [CrossRef]

14. Sanchez-Rivera, D.; Mohanty, K.; Balhoff, M. Reservoir simulation and optimization of huff-n-puff operations in the Bakken shale. *Fuel* **2015**, *147*, 82–94. [CrossRef]

15. Sun, J.; Zou, A.; Sotelo, E.; Schechter, D. Numerical simulation of CO_2 huff-n-puff in complex fracture networks of unconventional liquid reservoirs. *J. Nat. Gas Sci. Eng.* **2016**, *31*, 481–492. [CrossRef]

16. Yu, W.; Lashgari, H.R.; Wu, K.; Sepehrnoori, K. CO_2 injection for enhanced oil recovery in Bakken tight oil reservoirs. *Fuel* **2015**, *159*, 354–363. [CrossRef]

17. Sheng, J.J.; Chen, K. Evaluation of the EOR potential of gas and water injection in shale oil reservoirs. *J. Unconv. Oil Gas Resour.* **2014**, *5*, 1–9. [CrossRef]

18. Fathi, E.; Akkutlu, I.Y. Mass transport of adsorbed-phase in stochastic porous medium with fluctuating porosity field and nonlinear gas adsorption kinetics. *Transp. Porous Med.* **2012**, *91*, 5–33. [CrossRef]

19. Sun, H.; Yao, J.; Gao, S.; Fan, D.; Wang, C.; Sun, Z. Numerical study of CO_2 enhanced natural gas recovery and sequestration in shale gas reservoirs. *Int. J. Greenh. Gas Con.* **2013**, *19*, 406–419. [CrossRef]

20. Kalantari-Dahaghi, A. Numerical simulation and modeling of enhanced gas recovery and CO2 sequestration in shale gas reservoirs: A feasibility study. In Proceedings of the SPE International Conference on CO2, Capture, Storage, and Utilization, New Orleans, LA, USA, 10–12 November 2010.

21. Environment Protection Agency (EPA). Assessing the Emissions from the Oil and Gas Development in the Bakken Formation and Their Impact on Air Quality in National Parks. 2013. Available online: https://www.eenews.net/assets/2013/11/06/document_gw_01.pdf (accessed on 31 October 2018).

22. Prenni, A.J.; Day, D.E.; Evanoski-Cole, A.R.; Sive, B.C.; Hecobian, A.; Zhou, Y.; Gebhart, K.A.; Hand, J.L.; Sullivan, A.P.; Li, Y.; et al. Oil and gas impacts on air quality in federal lands in the Bakken region: An overview of the Bakken air quality study and first results. *Atmos. Chem. Phys.* **2016**, *16*, 1401–1416. [CrossRef]

23. Ratner, M.; Tiemann, M. An Overview of Unconventional Oil and Natural Gas: Resources and Federal Actions. Congressional Research Service Report. 2015. Available online: https://fas.org/sgp/crs/misc/R43148.pdf (accessed on 20 November 2018).

24. Energy Information Administration (EIA). Shale Oil and Shale Gas Resources Are Globally Abundant. 2013. Available online: https://www.eia.gov/todayinenergy/detail.php?id=11611 (accessed on 20 November 2018).

25. Energy Information Administration (EIA). World Shale Resource Assessments. 2015. Available online: https://www.eia.gov/analysis/studies/worldshalegas/ (accessed on 20 November 2018).

26. Energy Information Administration (EIA). Tight Oil Expected to Make Up Most of U.S. Oil Production Increase through 2040. 2017. Available online: https://www.eia.gov/todayinenergy/detail.php?id=29932 (accessed on 20 November 2018).

27. Sheng, J.J. Enhanced oil recovery in shale reservoirs by gas injection. *J. Nat. Gas Sci. Eng.* **2015**, *22*, 252–259. [CrossRef]

28. Wan, T.; Yu, Y.; Sheng, J.J. Experimental and numerical study of the EOR potential in liquid-rich shales by cyclic gas injection. *J. Unconv. Oil Gas Resour.* **2015**, *12*, 56–67. [CrossRef]

29. Song, C.; Yang, D. Experimental and numerical evaluation of CO_2 huff-n-puff processes in Bakken formation. *Fuel* **2017**, *190*, 145–162. [CrossRef]

30. Yang, D.Y.; Song, C.; Zhang, J.; Zhang, G.; Ji, Y.; Gao, J. Performance evaluation of injectivity for water-alternating-CO_2 processes in tight oil formations. *Fuel* **2015**, *139*, 292–300. [CrossRef]

31. Gamadi, T.D.; Sheng, J.J.; Soliman, M.Y. An experimental study of cyclic gas injection to improve shale oil recovery. In Proceedings of the SPE Annual Technical Conference and Exhibition, New Orleans, LA, USA, 30 September–2 October 2013.

32. Gamadi, T.D.; Sheng, J.J.; Soliman, M.Y.; Menouar, H.; Watson, M.C.; Emadibaladehi, H. An experimental study of cyclic CO_2 injection to improve shale oil recovery. In Proceedings of the SPE Improved Oil Recovery Symposium, Tulsa, OK, USA, 12–16 April 2014.

33. Adel, I.A.; Tovar, F.D.; Zhang, F.; Schechter, D.S. The impact of MMP on recovery factor during CO_2-EOR in Unconventional liquid reservoirs. In Proceedings of the SPE Annual Technical Conference and Exhibition, San Antonio, TX, USA, 24–26 September 2018.

34. Yu, W.; Lashgari, H.R.; Sepehrnoori, K. Simulation study of CO2 huff-n-puff process in Bakken tight oil reservoirs. In Proceedings of the SPE Western North American and Rocky Mountain Joint Meeting, Denver, CO, USA, 17–18 April 2014.

35. Zhang, Y.; Yu, W.; Li, Z.; Sepehrnoori, K. Simulation study of factors affecting CO_2 huff-n-puff process in tight oil reservoirs. *J. Pet. Sci. Eng.* **2018**, *163*, 264–269. [CrossRef]

36. Atan, S.; Ajayi, A.; Honarpour, M.; Turek, E.; Dillenbeck, E.; Mock, C.; Ahmadi, M.; Pereira, C. The viability of gas injection EOR in Eagle Ford shale reservoirs. In Proceedings of the SPE Annual Technical Conference and Exhibition, San Antonio, TX, USA, 24–26 September 2018.

37. Chen, C.; Balhoff, M.; Mohanty, K.K. Effect of reservoir heterogeneity on improved shale oil recovery by CO_2 huff-n-puff. In Proceedings of the Unconventional Resources Conference, The Woodland, TX, USA, 10–12 April 2013.

38. Sigmund, P.M. Prediction of molecular diffusion at reservoir conditions. Part I—measurement and prediction of binary dense gas diffusion coefficients. *J. Can. Pet. Technol.* **1976**, *15*, 48–57. [CrossRef]

39. Sigmund, P.M. Prediction of molecular diffusion at reservoir conditions. Part II—estimating the effects of molecular diffusion and convective mixing in multi-component systems. *J. Can. Pet. Technol.* **1976**, *15*, 53–62. [CrossRef]

40. Wilke, C.R.; Chang, P. Correlation of diffusion coefficients in dilute solutions. *AIChE J.* **1955**, *1*, 264–270. [CrossRef]

41. Du, F.; Nojabaei, B. Estimating diffusion coefficients of shale oil, gas, and condensate with nano-confinement effect. Presented at the 2019 Society of Petroleum Engineers Eastern Regional Meeting, Charleston, WV, USA, 15–17 October 2019, forthcoming.

42. Leahy-Dios, A.; Firoozabadi, A. Unified model for nonideal multicomponent molecular diffusion coefficients. *AIChE J.* **2007**, *53*, 2932–2939. [CrossRef]

43. Petersen, E.E. Diffusion in a pore of varying cross section. *AIChE J.* **1958**, *4*, 343–345. [CrossRef]

44. Epstein, N. On tortuosity and the tortuosity factor in flow and diffusion through porous media. *Chem. Eng. Sci.* **1989**, *44*, 777–779. [CrossRef]

45. Huang, J.; Xiao, F.; Dong, H.; Yin, X. Diffusion tortuosity in complex porous media from pore-scale numerical simulations. *Comput. Fluids* **2019**, *185*, 66–74. [CrossRef]

46. Ullman, W.J.; Aller, R.C. Diffusion coefficients in near shore marine sediments. *Limnol. Oceanogr.* **1982**, *27*, 552–556. [CrossRef]

47. Alavian, S.A. Modeling CO_2 Injection in Fractured Reservoirs Using Single Matrix Block System. Ph.D. Dissertation, Norwegian University of Science and Technology, Trondheim, Norway, 2011.

48. Atkins, E.R.; Smith, G.H. The significance of particle shape in formation resistivity factor porosity relationships. *J. Pet. Technol.* **1961**, *13*, 285–291. [CrossRef]

49. Alfarge, D.; Wei, M.; Bai, B. Mechanistic study for the applicability of CO_2-EOR in unconventional Liquids rich reservoirs. In Proceedings of the SPE Improved Oil Recovery Conference, Tulsa, OK, USA, 14–18 April 2018.

50. Teklu, T.W.; Alharthy, N.; Kazemi, H.; Yin, X.; Graves, R.M.; AlSumaiti, A.M. Phase behavior and minimum miscibility pressure in nanopores. *SPEREE* **2014**, *17*, 396–403. [CrossRef]

51. Zhang, K.; Nojabaei, B.; Ahmadi, K.; Johns, R.T. Minimum miscibility pressure calculation for oil shale and tight reservoirs with large gas–oil capillary pressure. In Proceedings of the Unconventional Resources Technology Conference, Houston, TX, USA, 23–25 July 2018.

52. Zhang, Y.; Di, Y.; Yu, W.; Sepehrnoori, K. A Comprehensive Model for Investigation of CO_2-EOR with Nanopore Confinement in the Bakken Tight Oil Reservoir. In Proceedings of the SPE Annual Technical Conference and Exhibition, San Antonio, TX, USA, 9–11 October 2017.

53. Jessen, K.; Orr, F.M. On interfacial-tension measurements to estimate minimum miscibility pressures. *SPEREE* **2008**, *11*, 933–939. [CrossRef]

54. Nojabaei, B.; Johns, R. T, Extrapolation of black- and volatile-oil fluid properties with application to immiscible/miscible gas injection. *J. Nat. Gas Sci. Eng.* **2016**, *33*, 367–377. [CrossRef]

55. Wang, S.; Ma, M.; Chen, S. Application of PC-SAFT equation of state for CO_2 minimum miscibility pressure prediction in nanopores. In Proceedings of the SPE Improved Oil Recovery Conference, Tulsa, OK, USA, 11–13 April 2016.

56. Huang, J.; Jin, T.; Chai, Z.; Barrufet, M.; Killough, J. Compositional simulation of fractured shale reservoir with distribution of nanopores using coupled multi-porosity and EDFM method. *J. Pet. Sci. Eng.* **2019**, *179*, 1078–1089. [CrossRef]

57. Du, F.; Nojabaei, B.; Johns, R.T. A black-oil approach to model produced gas injection for enhanced recovery of conventional and unconventional reservoirs. In Proceedings of the SPE Annual Technical Conference and Exhibition, Dallas, TX, USA, 24–26 September 2018.

58. Li, L.; Su, Y.; Sheng, J.J.; Hao, Y.; Wang, W.; Lv, Y.; Zhao, Q.; Wang, H. Experimental and numerical study on CO_2 sweep volume during CO_2 huff-n-puff enhanced oil recovery process in shale oil reservoirs. *Energy Fuels* **2019**, *33*, 4017–4032. [CrossRef]

59. Zuloaga, P.; Yu, W.; Miao, J.; Sepehrnoori, K. Performance evaluation of CO_2 huff-n-puff and continuous CO_2 injection in tight oil reservoirs. *Energy* **2017**, *134*, 181–192. [CrossRef]

60. Sun, R.; Yu, W.; Xu, F.; Pu, H.; Miao, J. Compositional simulation of CO_2 huff-n-puff process in Middle Bakken tight oil reservoirs with hydraulic fractures. *Fuel* **2019**, *236*, 1446–1457. [CrossRef]

61. Wang, L.; Yu, W. Mechanistic simulation study of gas puff and huff process for Bakken tight oil fractured reservoir. *Fuel* **2019**, *239*, 1179–1193. [CrossRef]

62. Yu, W.; Zhang, Y.; Varavei, A.; Sepehrnoori, K.; Zhang, T.; W, K.; Miao, J. Compositional simulation of CO_2 huff-n-puff in Eagle Ford tight oil reservoirs with CO_2 molecular diffusion, Nano pore confinement and complex natural fractures. In Proceedings of the SPE Improved Oil Recovery Conference, Tulsa, OK, USA, 14–18 April 2018.

63. Rassenfoss, S. Shale EOS Works, But Will It Make a Difference? JPT, 2017. Available online: https://www.spe.org/en/jpt/jpt-article-detail/?art=3391 (accessed on 20 November 2018).

64. Hoffman, B.T. Huff-n-Puff gas injection pilots projects in the Eagle Ford. In Proceedings of the SPE Canada Unconventional Resources Conference, Calgary, AB, Canada, 13–14 March 2018.

65. Jenkins, C.D.; Boyer, C.M. Coalbed- and shale-gas reservoirs. *J. Pet. Technol.* **2008**, *60*, 92–99. [CrossRef]

66. Ross, D.J.K.; Bustin, R.M. The importance of shale composition and pore structure upon gas storage potential of shale gas reservoirs. *Mar. Pet. Geol.* **2009**, *26*, 916–927. [CrossRef]

67. Energy Information Administration (EIA). Technology Drives Natural Gas Production Growth from Shale Gas Formations. 2011. Available online: https://www.eia.gov/todayinenergy/detail.php?id=2170 (accessed on 20 November 2018).

68. Energy Information Administration (EIA). Review of Emerging Resources: U.S. Shale Gas and Shale Oil Plays. 2011. Available online: https://www.eia.gov/analysis/studies/usshalegas/pdf/usshaleplays.pdf (accessed on 20 November 2018).

69. U.S. Geological Survey (USGS). USGS Estimates 304 Trillion Cubic Feet of Natural Gas in the Bossier and Haynesville Formations of the U.S. Gulf Coast. 2017. Available online: https://www.usgs.gov/news/usgs-estimates-304-trillion-cubic-feet-natural-gas-bossier-and-haynesville-formations-us-gulf (accessed on 20 November 2018).

70. Fayetteville Shale Natural Gas (FSNG). Available online: http://lingo.cast.uark.edu/LINGOPUBLIC/about/ (accessed on 20 November 2018).

71. Energy Information Administration (EIA). Coal Production and Prices Decline in 2015. 2016. Available online: https://www.eia.gov/todayinenergy/detail.php?id=24472 (accessed on 20 November 2018).

72. Baihly, J.; Altman, R.; Malpani, R.; Luo, F. Shale gas production decline trend comparison over time and basins. In Proceedings of the SPE Annual Technical Conference and Exhibition, Florence, Italy, 19–22 September 2010.

73. Busch, A.; Alles, S.; Gensterblum, Y.; Prinz, D.; Dewhurst, D.N.; Raven, M.D.; Stanjek, H.; Krooss, B.M. Carbon dioxide storage potential of shales. *Int. J. Greenh. Gas Con.* **2008**, *2*, 297–308. [CrossRef]

74. Chen, T.Y.; Feng, X.; Pan, Z. Experimental study on kinetic swelling of organic-rich shale in CO_2, CH_4, and N_2. *J. Nat. Gas Sci. Eng.* **2018**, *55*, 406–417. [CrossRef]

75. Pan, Y.; Hui, D.; Luo, P.; Zhang, Y.; Sun, L.; Wang, K. Experimental investigation of the geochemical interactions between supercritical CO_2 and shale: Implications for CO_2 storage in gas-bearing shale formations. *Energy Fuels* **2018**, *32*, 1963–1978. [CrossRef]

76. Yuan, W.; Pan, Z.; Li, X.; Yang, Y.; Zhao, C.; Connell, L.D.; Li, S.; He, J. Experimental study and modeling of methane adsorption and diffusion in shale. *Fuel* **2014**, *117*, 509–519. [CrossRef]

77. Heller, R.; Zoback, M. Adsorption of methane and carbon dioxide on gas shale and pure mineral samples. *J. Unconv. Oil Gas Resour.* **2014**, *8*, 14–24. [CrossRef]

78. Chareonsuppanimit, P.; Mohammad, S.A.; Robinson, R.L., Jr.; Gasem, K.A.M. High-pressure adsorption of gases on shales: Measurements and modeling. *Int. J. Coal. Geol.* **2012**, *95*, 34–46. [CrossRef]

79. Chen, T.Y.; Feng, X.; Pan, Z. Experimental study of swelling of organic rich shale in methane. *Int. J. Coal. Geol.* **2015**, *150*, 64–73. [CrossRef]

80. Lu, Y.; Ao, X.; Tang, J.; Jia, Y.; Zhang, X.; Chen, Y. Swelling of shale in supercritical carbon dioxide. *J. Nat. Gas Sci. Eng.* **2016**, *30*, 268–275. [CrossRef]

81. Yang, B.; Kang, Y.; You, L.; Li, X.; Chen, Q. Measurement of the surface diffusion coefficient for adsorbed gas in the fine mesopores and micropores of shale organic matter. *Fuel* **2016**, *181*, 793–804. [CrossRef]

82. Ao, X.; Lu, Y.; Tang, J.; Chen, Y.; Li, H. Investigation on the physics structure and chemical properties of the shale treated by supercritical CO_2. *J. CO2 Util.* **2017**, *20*, 274–281. [CrossRef]

83. Nuttal, B.C. Reassessment of CO_2 sequestration capacity and enhanced gas recovery potential of Middle and Upper Devonian Black Shales in the Appalachian Basin. In Proceedings of the MRCSP Phase II Topical Report, 2005 October–2010 October, Kentucky Geological Survey, Lexington, Kentucky, 2010. Available online: https://irp-cdn.multiscreensite.com/5b322158/files/uploaded/topical_4_black_shale.pdf (accessed on 20 November 2018).

84. Sondergeld, C.H.; Newsham, K.E.; Comisky, J.T.; Rice, M.C.; Rai, C.S. Petrophysical considerations in evaluating and producing shale gas resources. In Proceedings of the SPE Unconventional Gas Conference, Pittsburgh, PA, USA, 23–25 February 2010.

85. Wu, K.; Li, X.; Wang, C.; Yu, W.; Chen, Z. Model for surface diffusion of adsorbed gas in nanopores of shale gas reservoirs. *Ind. Eng. Chem. Res.* **2015**, *54*, 3225–3236. [CrossRef]

86. Chio, J.G.; Do, D.D.; Do, H.D. Surface diffusion of adsorbed molecules in porous media: Monolayer, multilayer, and capillary condensation regimes. *Ind. Eng. Chem. Res.* **2001**, *40*, 4005–4031. [CrossRef]

87. Kang, S.M.; Fathi, E.; Ambrose, R.J.; Akkutlu, I.Y.; Sigal, R.F. Carbon dioxide storage capacity of organic-rich shales. *SPE J.* **2011**, *16*, 842–855. [CrossRef]

88. Godec, M.; Koperna, G.; Petrusak, R.; Oudinot, A. Potential for enhanced gas recovery and CO_2 storage in the Marcellus shale in the Eastern United States. *Int. J. Coal Geol.* **2013**, *118*, 95–104. [CrossRef]

89. Yu, W.; Al-Shalabi, E.W.; Sepehrnoori, K. A sensitivity study of potential CO_2 injection for enhanced gas recovery in Barnett shale reservoirs. In Proceedings of the SPE Unconventional Resources Conference, The Woodlands, TX, USA, 1–3 April 2014.

90. Kim, T.H.; Park, S.S.; Lee, K.S. Modeling of CO_2 injection considering multi-component transport and geotechnical effect in shale gas reservoirs. In Proceedings of the SPE/IATMI Asia Pacific Oil & Gas Conference and Exhibition, Bali, Indonesia, 20–22 October 2015.

91. Eshkalak, M.O.; Al-Shalabi, E.W.; Sanaei, A.; Aybar, U.; Sepehrnoori, K. Enhanced gas recovery by CO_2 sequestration versus re-fracturing treatment in unconventional shale gas reservoirs. In Proceedings of the Abu Dhabi International Petroleum Exhibition and Conference, Abu Dhabi, UAE, 10–13 November 2014.

92. Abba, M.K.; Al-Othaibi, A.; Abbas, A.J.; Nasr, G.G.; Mukhtar, A. Experimental investigation on the impact of connate water salinity on dispersion coefficient in consolidated rocks cores during enhanced gas recovery by CO_2 injection. *J. Nat. Gas Sci. Eng.* **2018**, *60*, 190–201. [CrossRef]

93. Fathi, E.; Akkutlu, I.Y. Matrix heterogeneity effects on gas transport and adsorption in coalbed and shale gas reservoirs. *Transp. Porous Med.* **2009**, *80*, 281–304. [CrossRef]

94. Jia, B.; Tsau, J.B.; Barati, R. Role of molecular diffusion in heterogeneous, naturally fractured shale reservoirs during CO_2 huff-n-puff. *J. Nat. Gas Sci. Eng.* **2018**, *164*, 31–42. [CrossRef]

95. Honari, A.; Bijeljic, B.; Johns, M.L.; May, E.F. Enhanced gas recovery with CO_2 sequestration: The effect of medium heterogeneity on the dispersion of supercritical CO_2–CH_4. *Int. J. Greenh. Gas Con.* **2015**, *39*, 39–50. [CrossRef]

96. Tao, Z.; Clarens, A. Estimating the carbon sequestration capacity of shale formations using methane production rates. *Environ. Sci. Technol.* **2013**, *47*, 11318–11325. [CrossRef]

97. Edwards, R.W.; Celia, M.A.; Bandilla, K.W.; Doster, F.; Kanno, C.M. A model to estimate carbon dioxide injectivity and storage capacity for geological sequestration in shale gas well. *Environ. Sci. Technol.* **2015**, *49*, 9222–9229. [CrossRef] [PubMed]

98. Nuttall, B.C.; Eble, C.F.; Drahovzal, J.A.; Bustin, R.M. Analysis of Devonian Black Shales in Kentucky for potential carbon dioxide sequestration and enhanced natural gas production. In *Greenhouse Gas Control Technologies 7*; Report Kentucky Geological Survey/University of Kentucky (DE-FC26-02NT41442); Elsevier Science Ltd.: Amsterdam, The Netherlands, 2005.

99. Louk, K.; Ripepi, N.; Luxbacher, K.; Gilliland, E.; Tang, X.; Keles, C.; Schlosser, C.; Diminick, E.; Keim, S.; Amante, J.; et al. Monitoring CO_2 storage and enhanced gas recovery in unconventional shale reservoirs: Results from the Morgan County, Tennessee injection test. *J. Nat. Gas Sci. Eng.* **2017**, *45*, 11–25. [CrossRef]

100. Fuel Fix. Midstream Firms Build to Meet Eagle Ford Condensate Production. 2014. Available online: http://fuelfix.com/blog/2014/09/03/midstream-firms-build-to-meet-eagle-ford-condensate-production/ (accessed on 20 November 2018).

101. Sigmund, P.M.; Dranchuk, P.M.; Morrow, N.R.; Purvis, P.A. Retrograde condensation in porous media. *SPE J.* **1973**, *13*, 93–104. [CrossRef]

102. Al-Anazi, H.A.; Aramco, S.; Pope, G.A.; Sharma, M.M.; Metcalfe, R.S. Laboratory measurements of condensate blocking and treatment for both low and high permeability rocks. In Proceedings of the SPE Annual Technical Conference and Exhibition, San Antonio, TX, USA, 29 September–2 October 2002.

103. Meng, X.; Sheng, J.J. Experimental study on revaporization mechanism of huff-n-puff gas injection to enhance condensate recovery in shale gas condensate reservoirs. In Proceedings of the SPE Improved Oil Recovery Conference, Tulsa, OK, USA, 11–13 April 2016.

104. Meng, X.; Sheng, J.J. Optimization of huff-n-puff gas injection in a shale gas condensate reservoir. *J. Unconv. Oil Gas Resour.* **2016**, *16*, 34–44. [CrossRef]

105. Sheng, J.J.; Mody, F.; Griffith, P.J.; Barnes, W.N. Potential to increase condensate oil production by huff-n-puff gas injection in a shale condensate reservoir. *J. Nat. Gas Sci. Eng.* **2016**, *28*, 46–51. [CrossRef]

106. Jiang, J.; Younis, R.M. Compositional modeling of enhanced hydrocarbons recovery for fractured shale gas-condensate reservoirs with the effects of capillary pressure and multicomponent mechanisms. *J. Nat. Gas Sci. Eng.* **2016**, *34*, 1262–1275. [CrossRef]

107. Sheng, J.J. Increase liquid oil production by huff-n-puff of produced gas in shale gas condensate reservoirs. *J. Unconv. Oil Gas Resour.* **2015**, *11*, 19–26. [CrossRef]

108. Sharma, S.; Sheng, J.J. A comparative study of huff-n-puff gas and solvent injection in a shale gas condensate core. *J. Nat. Gas Sci. Eng.* **2017**, *38*, 549–565. [CrossRef]

109. Nojabaei, B.; Johns, R.T.; Chu, L. Effect of Capillary Pressure on Phase Behavior in Tight Rocks and Shales. *SPEREE* **2013**, *16*, 281–289. [CrossRef]

110. Raupach, M.R.; Marland, G.; Ciais, P.; Quere, C.L.; Canadell, J.G.; Klepper, G.; Field, C.B. Global and regional drivers of accelerating CO_2 emissions. *Proc. Natl. Acad. Sci. USA* **2007**, *104*, 10288–10293. [CrossRef] [PubMed]

111. Barrufet, M.A.; Bacquet, A.; Falcone, G. Analysis of the storage capacity for CO_2 sequestration of a depleted gas condensate reservoir and a saline aquifer. *J. Can. Pet. Technol.* **2010**, *49*, 23–31. [CrossRef]

112. Howarth, R.W.; Santoro, R.; Ingraffea, A. Methane and the greenhouse-gas footprint of natural gas from shale formations. *Clim. Chang.* **2011**, *106*, 679–690. [CrossRef]

113. Energy Information Administration (EIA). North Dakota Natural Gas Flaring Targets Challenged by Rapid Production Growth. 2015. Available online: https://www.eia.gov/todayinenergy/detail.php?id=23752 (accessed on 20 November 2018).

114. Ghaderi, S.M.; Clarkson, C.R.; Ghanizadeh, A.; Barry, K.; Fiorentino, R. Improved oil recovery in tight oil formations: Results of water injection operations and gas injection sensitivities in the Bakken formation of Southeast Saskatchewan. Presented at the SPE Unconventional Resources Conference, Calgary, AB, Canada, 15–16 February 2017.

115. Energy Information Administration (EIA). Natural Gas Vented and Flared (Summary). 2019. Available online: https://www.eia.gov/dnav/ng/NG_SUM_LSUM_A_EPG0_VGV_MMCF_A.htm (accessed on 30 April 2019).

116.　Hughes, L. Biological consequences of global warming: Is the signal already apparent? *Trends Ecol. Evol.* **2000**, *15*, 56–61. [CrossRef]

117.　Pu, H.; Wang, Y.; Li, Y. How CO_2-storage mechanisms are different in organic shale: Characterization and simulation studies. *SPE J.* **2017**, *23*, 661–671. [CrossRef]

118.　Middleton, R.; Viswanathan, H.; Currier, R.; Gupta, R. CO_2 as a fracturing fluid: Potential for commercial-scale shale gas production and CO_2 sequestration. *Energy Proced.* **2014**, *63*, 7780–7784. [CrossRef]

119.　Harris, P.C.; Haynes, R.J.; Egger, J.P. The use of CO_2-based fracturing fluids in the Red Fork formation in the Anadarko basin, Oklahoma. *J. Pet. Technol.* **1984**, *36*, 1–003. [CrossRef]

120.　Gandossi, L. An overview of hydraulic fracturing and other formation stimulation technologies for shale gas production. In *Joint Research Centre of the European Commission*; Scientific and Policy Report; Publications Office of the European Union: Luxembourg, 2013.